PHILOSOPHICAL TRANSACTIONS OF THE ROYAL SOCIETY A MATHEMATICAL, PHYSICAL & ENGINEERING SCIENCES

The Excitation Functions of Ba (p, X) $^{\text{M}}$Xe (M = 124-136) in the Energy Range 38-600 MeV; The Use of 'Cosmogenic' Xenon for Estimating 'Burial' Depths and 'Real' Exposure Ages

W. A. Kaiser

Phil. Trans. R. Soc. Lond. A 1977 **285**, 337-362
doi: 10.1098/rsta.1977.0074

Phil. Trans. R. Soc. Lond. A. **285**, 337–362 (1977) [337]
Printed in Great Britain

The excitation functions of Ba (p, X) ^{M}Xe (M = 124–136) in the energy range 38–600 MeV; the use of 'cosmogenic' xenon for estimating 'burial' depths and 'real' exposure ages

By W. A. Kaiser†
Institut für Kernchemie, der Universität Köln, Zülpicher Strasse 47,
5000 *Köln* 41, *Germany*

Thin target experiments were performed to obtain the excitation functions of the reactions Ba (p, X) ^{M}Xe. The abundances of all stable Xe isotopes and of the radionuclides ^{127}Xe and ^{131}Ba were determined by means of rare gas mass spectroscopy and γ-counting, respectively. The excitation functions show marked characteristics leading to strong variations in the proton-induced Xe-ratios as functions of energy. The ^{131}Xe/^{126}Xe ratio – the special lunar anomaly – was found to vary from 1.14 ± 0.4 (600 MeV) to 248.8 ± 4.0 (75 MeV). The ^{M}Xe production rates and the ^{M}Xe/^{126}Xe ratios as functions of depths were estimated for 2π geometry utilizing the depth dependent galactic-cosmic-ray (g.c.r.) fluxes of Reedy & Arnold (1972). Substantial isotopic variations for all of the proton-induced Xe ratios were found, sufficient to explain most of the cosmogenic Xe ratios (exceptions are ^{130}Xe, and ^{132}Xe) measured yet in lunar samples with proton-induced reactions on Ba at different depths in the Moon. Actual lunar samples are used to check the validity of the results.

Introduction

Goles & Anders (1961) suggested that high energy cosmic ray particles (g.c.r.) produced the 'secondary' anomalies observed in the Xe spectra measured by Reynolds (1960*a*, *b*) and his co-workers (e.g. Krummenacher *et al.* 1962). Since then several investigations have been performed to establish the presence of a spallogenic or more comprehensively 'cosmogenic' Xe component, whereby the word 'cosmogenic' is a collective name for nuclei produced by the primary and the secondary component of the g.c.r. (see Rowe *et al.* 1965; Merrihue 1966; Pepin 1966; Marti *et al.* 1966; Rowe & Bogard 1966; Rowe *et al.* 1966; Rowe 1967; Hohenberg *et al.* 1967; Clark *et al.* 1967; Funk *et al.* 1967; Hohenberg & Rowe 1970; Kaiser 1971; Burnett *et al.* 1971; Huneke *et al.* 1972; Kaiser & Rajan 1973).

The contribution of a 'cosmogenic' Xe component in most of the meteoritic samples is relatively small. Therefore, the extraction of a pure 'cosmogenic' Xe component is rather difficult. The situation is different in lunar samples. The absence of the expected 'special' anomalies originating from extinct radionuclides like ^{129}I, ^{244}Pu or even more exotic elements made the lunar samples more interesting for the study of the cosmogenic Xe component. This interest was especially advanced by the occurrence of the ^{131}Xe enrichment (Hohenberg *et al.* 1970; Marti *et al.* 1970; Pepin *et al.* 1970; Albee *et al.* 1970), an effect seen only one time before (Pepin 1966). Thus, a large number of lunar samples were studied and cosmogenic Xe spectra of quite distinct isotopic composition were derived (e.g. Hohenberg *et al.* 1970; Bogard *et al.* 1971; Marti & Lugmair 1971; Kaiser 1971). Although the large spread, as observed in the cosmogenic

† Present address: Wasserturmstrasse 22, 6901 Eppelheim, West Germany.

$^{131}Xe/^{126}Xe$ ratio, was not found among the other cosmogenic $^{M}Xe/^{126}Xe$ ratios rather pronounced isotopic differences were established demonstrating the complexity of that particular Xe component.

Experimental

Natural barium in form of pure $BaCl_2$ (Merck p.a.) was used as target material. In order to avoid weighing errors due to the hygroscopic nature of the $BaCl_2$ compound and to get rid of any inherited Xe contamination several grams of the material were preheated in a quartz tube under high vacuum (10^{-7} Torr; 10^{-5} Pa) to 1050 °C (well beyond the melting point of $BaCl_2$: 925–963 °C). The $BaCl_2$ compound was kept at this temperature for *ca.* 1 h. After complete degassing the quartz tube was sealed off under vacuum. The ampule was then transferred to a glove-box where it was cracked under a nitrogen atmosphere. The molten $BaCl_2$ blocks were crushed to small pieces. Only millimetre-size crystals were chosen as probe material. The sample preparation and weighing procedure were also performed in the glove box.

The proton irradiations were executed at the Research Centers of Orsay (internal proton-beam facility of the 152 MeV Synchro-cyclotron at the Institut de Physique Nucléaire Orsay; available proton-energy 38–150 MeV) and Genève (internal proton-beam facility at the 600 MeV Synchro-cyclotron at the Centre Européenne Recherche Nucléaire [CERN]; available proton-energy 150–600 MeV).

Due to the chemical characteristics of the target material, $BaCl_2$, and the irradiation conditions mentioned below, two serious experimental difficulties were encountered: 'thermal heating' during the irradiation and 'leaching out' of Xe after the irradiation.

Thermal heating

The target holders for internal irradiations are standardized in both institutions. Due to the very small geometrical cross section of the proton-beam inside of such a machine, the effective area of an inserted target is rather small (*ca.* 3 mm in radial direction and *ca.* 115 mm in vertical direction, whereby the optimal position in vertical direction is energy dependent due to the oscillation of the particle-beam during acceleration). The aperture available for introducing 'thin target' arrangements is therefore small (*ca.* 50 mm in diameter in both institutions). This restricted at first the use of quartz encapsulated $BaCl_2$ samples. Slightly modified, but still conventional types of target holders were used (figures 1 *a*, *b*, and 2 *a*). Sticking to the chronology, the CERN experiments will be discussed first. The available space for filling in the target material was 2 mm × 2 mm × 20 mm. This space was then closely covered by an extremely pure (99.9999 % Al) 200 μm thick Al foil which served as sample cover, proton-flux monitor target, and as heat conducting material. The well known nuclear reaction ^{27}Al (p, 3p3n) ^{22}Na was employed for estimating the proton-flux. For determining the 'effective' proton-flux, only the shaded areas (figures 1 and 2) of the Al foils were used. The proton-flux values for these samples were independently determined. (Estimates of the range and the stopping power of the thin target experimental arrangements for the proton-energies concerned were obtained by using the tables of Williamson *et al.* (1966).) The attenuation of the energy of the protons passing through the experimental arrangements was rather small (< 2 MeV). Since the shape of the excitation curve of the monitor reaction ^{27}Al (p, 3p3n) ^{22}Na is relatively smooth in that energy range, the cross section was assumed to be the same for both Al samples. The proton-fluxes given

in table 2 are thus the averaged proton-fluxes for those two Al probes employing the ^{22}Na cross section of the proton-energy at the side of incidence. γ-autoradiographic investigations were carried out of all Al-foils showing that the $BaCl_2$ targets had really received most of the proton-dose. Thus, the danger of associating an incorrect proton-flux value to the proton-induced Xe amounts which could have been introduced by cutting out the two monitor Al foils was minimized. For the first series of experiments the target holders used were conventional

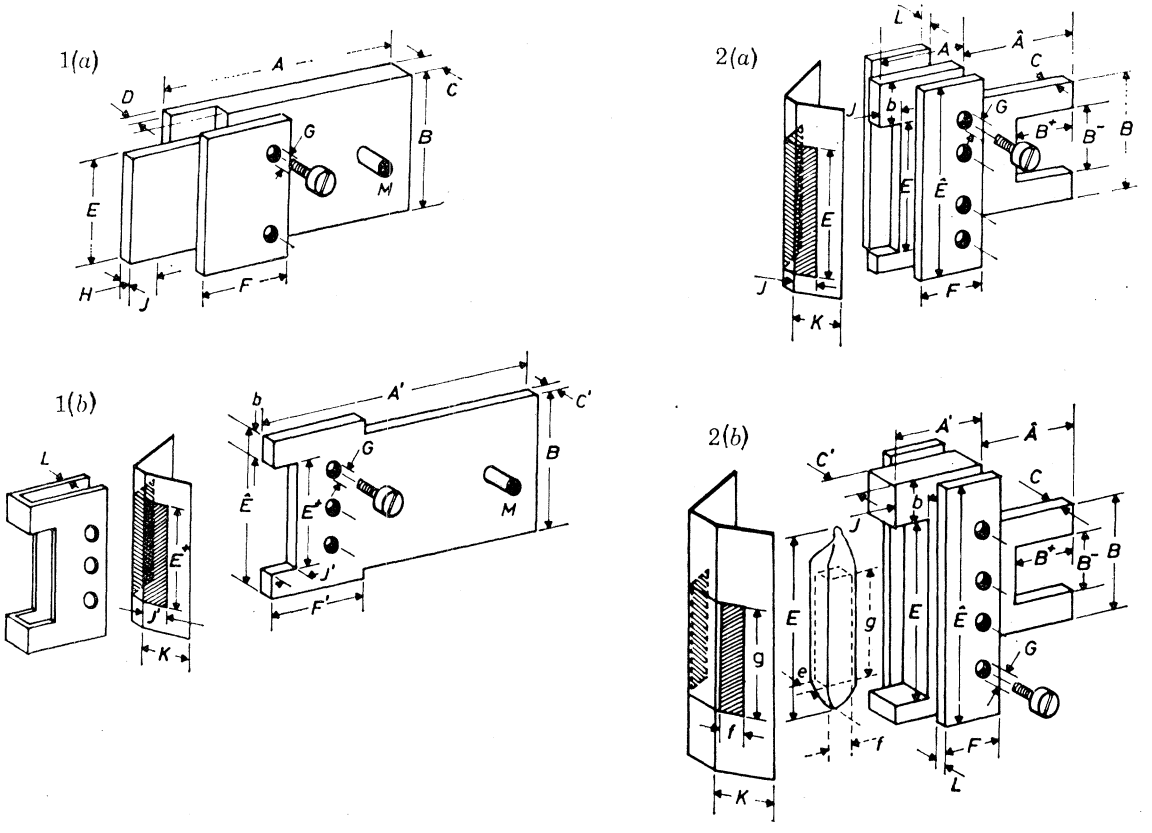

FIGURE 1. (*a*) Conventional CERN target holder for internal irradiation; all parts are made of pure Al; measures are: A (overall length) = 70 mm, B (overall height) = 30 mm, C (overall width = 3 mm, D = 1 mm, E (height of the actual target, surrounded by a monitor foil, e.g. Al-foil) = 30 mm, H (width of the actual target) = 3 mm, J (effective depth of the actual target) = 5 mm, F (width of the Al-plate to keep the target in place, tightened by 2 Al-screws) = 15 mm, G = 3 mm, M = pin for clamping the strongly activated target holder with an extension rod after the irradiation. (*b*) Modified CERN target holder; all parts are made of pure Al; measures are: A' = 75 mm, B = 30 mm, C' = 2 mm, $\hat{E}$ = 40 mm, E^{+} = 20 mm, $b = \hat{E} - E^{+} = 5 - 15$ mm depending upon the p-energy (see text), F' = 20 mm, G = 3 mm, J' = 2 mm, K (side length of the Al-cover-foil) = 10 mm, L = wall-thickness of the clamp for pressing the Al-foil against the target holder in order to conduct the thermal heat and to keep the space containing the $BaCl_2$ crystals tightly closed) = 1 mm.

FIGURE 2. (*a*) Modified Orsay target holder; all parts are made of pure Al; measures are: A = 15 mm, $\hat{A}$ = 15 mm, B = 32 mm, B^{+} = 12 mm, B^{-} = 12 mm, C = 2 mm, E = 20 mm, $\hat{E}$ = 40 mm, $b = \hat{E} - E = 2 - 18$ mm, F = 10 mm, G = 3 mm, J = 3 mm, K = 8 mm (Al-foil = 200 μm), L = 1 mm. (*b*) Strongly modified Orsay target holder; all parts are made of pure Al; Measures are: A' = 18 mm, $\hat{A}$ = 15 mm, B = 32 mm, B^{+} = 12 mm, B^{-} = 12 mm, C = 2 mm, C' = 4 mm, E = 33 mm, $\hat{E}$ = 45 mm, $b = \hat{E} - E = 2 - 10$ mm, F = 10 mm, G = 3 mm, J = 5 mm, K = 10 mm; measures of the quartz-ampulla: E (overall length) = 33 mm, e (inside dimension along the p-beam) = 2 mm, f (inside dimension perpendicular to the p-beam) = 3 mm, g (height of the $BaCl_2$-filling) $\leqslant$ 20 mm. Thickness of the quartz-ampulla walls $\sim$1 mm. Thickness of the Al-foil = 300 μm.

CERN manufactured ones (figure 1*a*) employing a 100 μm thick Al foil as cover. The irradiation time was 20 min each. The $BaCl_2$ compound was found to be severely damaged by 'thermal heating' leading probably to diffusive losses of a fraction of the Xe isotopes and of the more volatile members of the diverse isobars produced directly during the proton-exposure. Estimates of the isotopic Xe contributions produced during an irradiation of 5 min are given in table 1 for a proton-energy of 100 MeV and the target ^{138}Ba (71.66 % in natural barium) employing the Rudstam (1966) formula. Although the formula is rather inaccurate in estimating spallogenic Xe spectra in the case of the Ba–Xe-system due to the very small ΔA from target to product, the fraction of the directly produced Xe isotopes belonging to the respective isobars can be estimated quite well. After several test experiments with shorter irradiation times and slightly modified target holders to obtain better heat-conducting characteristics, we chose an irradiation time of 2 min and the target holder geometry displayed in figure 1*b*. Visual examination of the $BaCl_2$ crystals under a microscope after the proton-bombardment did not show any visible damage due to 'thermal heating'.

TABLE 1. FRACTIONS OF THE Xe ISOTOPES PRODUCED DURING A 5 MIN EXPOSURE OF Ba TARGETS TO PROTONS OF 100 MeV, ESTIMATED UTILIZING THE RUDSTAM FORMULA IDED-G (ISOTOPIC DISTRIBUTION AND ELEMENTAL DISTRIBUTION; GAUSS APPROXIMATION)

isotope	^{124}Xe	^{126}Xe	^{127}Xe	^{128}Xe	^{129}Xe	^{130}Xe	^{131}Xe	^{132}Xe	^{134}Xe	^{136}Xe
fraction of 'total' production	1.0	0.71	0.05	0.19	0.006	0.05	0.0005	0.03	0.98	1.0

In case of the Orsay thin target experiments the situation was more complicated due to the much higher flux of the internal proton-beam. In course of the experiments performed there 'effective' proton-fluxes up to 5×10^{14} p/s were measured. At CERN, the maximum proton-flux value observed was 1.48×10^{12} p/s for the 500 MeV proton-exposure. The attempt was made to operate the synchro-cyclotron with reduced proton-intensity but it turned out to be rather difficult and it was not really successful. In addition, difficulties with the pump system of the synchro-cyclotron occurred during irradiation, as a result of outgassing or evaporation of the $BaCl_2$ compound. This caused an automatic shut down of the proton-beam. These interruptions and the suspected variations of the production rates of the diverse Xe-isotopes in that energy range made us choose irradiation times of 5 min. Visual control of the $BaCl_2$ probe after this irradiation time did not show any signs of damage due to thermal heating for most of the samples. Exception was the 50 MeV probe where some of the $BaCl_2$ evaporated and precipitated on the Al foil. The measurement was disregarded. The inferred excitation functions showed for most of the Xe isotopes reasonably looking shapes, whereas those representing ^{130}Xe, ^{132}Xe and ^{134}Xe exhibited somewhat unusual patterns. Their patterns were marked by pronounced minimas in the energy range around 125 MeV where the other excitation functions displayed relatively strong enhancements or even maximum values. Because of this strange behaviour we repeated the measurements in this important energy range. Due to the problem of 'thermal heating' extensive modifications of the thin target arrangement had to be carried out. Special small quartz containers were designed to avoid the diffusive loss of any of the decay members of the diverse isobars.

The containers were made by inserting metallic Mo pieces of the dimensions 2 mm × 3 mm × 20 mm into quartz-tubing of *ca.* 3 mm inside diameter and heating the configuration till the

quartz softened and could be pressed around the Mo. In this way containers with perfect rectangular inside dimensions resulted. Afterwards these quartz containers were grinded in order to obtain also rectangular external dimensions with 1 mm wall thickness. The metallic Mo was then dissolved in a mixture of boiling HCl and HNO_3. Vacuum molten $BaCl_2$ crystals were filled into the ampules which then were attached to a high vacuum system. The $BaCl_2$ compound was again molten under high vacuum so that the molten liquid completely fills the volume of the containers. It was kept at 1050 °C for 1 h at a pressure of *ca.* 10^{-5} Pa. The containers were then sealed shortly above the surface of the probe material under vacuum without evaporating the material. The total lengths of those ampules did not exceed 33 mm. They were then mounted on the target holders (figure 2*b*) and covered with a 300 μm thick pure (99.999 %) Al foil which turned out to be necessary to conduct the thermal heat interjected.

Leaching

This concerns only the samples not encapsulated in quartz. The two-stage decay of the isobar 131 $^{131}\mathrm{Ba} \xrightarrow{12.0\mathrm{d}} {}^{131}\mathrm{Cs} \xrightarrow{9.7\mathrm{d}} {}^{131}\mathrm{Xe}$ requires roughly 2 months storage of the samples for decaying. As far as the CERN samples were concerned the storage time was even longer due to failures in the analysing system. During this storage time the samples got hydrated as was found out by re-weighing them. In order to get rid of this contamination, the samples were preheated in a quartz finger at 150 °C for 1 h in an auxiliary pump system which was directly connected to the sample system of the mass spectrometer by an ultra high vacuum valve. After sealing off the auxiliary pump line, the separating valve was opened and the Xe was extracted by heating the $BaCl_2$ compound to 1050 °C for 30 min. The temperature during this time was controlled by a Pt–Rh-thermocouple. The concentration of the mass spectroscopically determined ^{127}Xe activity corrected for the corresponding decrease due to the elapsed decay-time, showed rather large discrepancies with the values obtained by γ-counting which was performed a few days after the respective irradiations. The most plausible explanation is that, due to the water incorporation into the samples under study, structural changes in the $BaCl_2$ lattice might have occurred. During the preheating procedure the water was driven off causing a partial loss of the Xe. This remark is based upon the following experiment. In view of the recently discovered epithermal resonances of the ^{130}Ba (n, γ) ^{131}Xe reaction we redetermined the cross section of this reaction at thermal energy (10.5 barn at 'thermal energy'). For that purpose we had used vacuum molten $BaCl_2$ which was sealed in quartz ampules under vacuum. Exposing one of those samples to water vapour for some time and treating it the way we did with the thin target samples led to the same observation of substantial loss of xenon. This process explains also the higher Xe loss of the CERN samples compared to the Orsay samples since the CERN samples were stored for a longer time. Therefore, the cross section values given in this work are exclusively based upon the γ-counting of the ^{127}Xe activities and the ^{M}Xe/^{127}Xe ratios determined mass spectroscopically.

For γ-counting a 25 cm^3 Ge(Li)-detector with a resolution of 2.5 keV/channel was used. The efficiency of the γ-counter was determined for the γ-lines 203 keV (^{127}Xe), 496 keV (^{131}Ba) and 1275 keV (^{22}Na) employing several calibrated standards like ^{22}Na, ^{57}Co, ^{137}Cs, and ^{166}Ho with individual uncertainties smaller than 3 %. Despite this an error of 10 % in the efficiency was always assigned due to the slightly different geometrical shapes of standards and

samples. Additionally, the statistical error of the γ-counting was considered, where no errors were assumed for: ^{22}Na cross section from ^{27}Al, irradiation times, absolute yields of the diverse γ-lines, and the sample mass. The following physical constants were used: half-life of ^{22}Na = 2.62 a; of ^{127}Xe = 36.4 d; and of ^{131}Ba = 12.0 d; absolute yields of the γ-lines ^{22}Na (1275 keV) = 99 %, ^{127}Xe (203 keV) = 65 % (Meixner 1969), and ^{131}Ba (496 keV) = 48 % (Lederer 1967).

The quartz encapsulated $BaCl_2$ probes were loaded into the sample system after 2 months and were then (samples still encapsuled) heated to 1100 °C by means of a resistor oven. Then a complete Xe analysis was performed. This was done in the case that the ampule might have cracked and due to the heating consequently the gas would have leaked out and have been lost. Fortunately, none of the ampules cracked during the heating procedure. Permitting considerable time for cooling and re-establishing good vacuum conditions (12 h) the quartz containers were transported on a magnetized Ni plate inside of the sample system to a cracking device where the ampule was destroyed. The gas was then let into the cleaning part of the sample system. Due to this procedure and the high proton-dose received by the targets, the yields of all Xe isotopes, including ^{136}Xe, produced by the proton-bombardment could be determined. Blank runs performed under identical experimental conditions showed much lower abundance levels than observed in the irradiated samples (table 4). The ^{127}Xe concentrations determined via γ-counting was always in good agreement with the mass-spectrometrically obtained concentrations.

The 'effective' proton-fluxes were again estimated by taking the average of the two Al foil pieces due to the reasons given before. The situation was more intricate for the proton-flux estimation of the 38 MeV measurement due to the fact that the shape of the excitation function of ^{27}Al (p, 3p3n) ^{22}Na drops off steeply for energies smaller than 40 MeV.

Deviations of the horizontal positioning of the thin target arrangement relative to the proton-beam results in the target receiving protons of different energy (5 mm in radial distance corresponds to 1 MeV). In our case the extension of the arrangement was well defined and the positioning could be done accurately ($\pm$ 0.1 mm). Therefore, this error can be neglected. The more cardinal uncertainty was introduced by the attenuation of the proton-energy within the experimental arrangement. Here is about 5 MeV difference between the incidence side and the emerging side with reference to the beam. Assuming that the energy of the protons at incidence side was 38 MeV, the change of the cross section of the monitor reaction is about an order of magnitude when compared with that of the emerging side. Due to these difficulties the proton-flux listed for the 38 MeV irradiation is entirely based upon the measurement of the Al foil facing the beam leading to a slight overestimation of the 'effective' proton-flux values.

Results

The results are presented in tables 2–4. Table 2 contains the proton-energy in MeV, the mass of the $BaCl_2$ samples, the proton-fluxes, the fractional loss of Xe caused by leaching, the cross sections of ^{127}Xe determined by γ-counting, the cross sections of the monitor reaction used (^{27}Al (p, 3p3n) ^{22}Na), and the rough Xe data corrected for mass discrimination. Table 3 lists the ^{M}Xe/^{126}Xe ratios which are mainly proton-induced. In case of the $BaCl_2$ samples, not encapsulated in quartz, they were estimated assuming that all ^{136}Xe is from atmospheric contamination. The proton-induced ^{136}Xe yield is assumed to be zero. The proton-induced ^{126}Xe

PHILOSOPHICAL TRANSACTIONS OF THE ROYAL SOCIETY A MATHEMATICAL, PHYSICAL & ENGINEERING SCIENCES

TABLE 2

energy / MeV	mass [$BaCl_2$] / g	10^{-12} p-flux / cm^{-2} s^{-1}	fraction lost Xe	(^{127}Xe) / mbarn	(^{22}Na) / mbarn	xenon: ^{124}Xe/^{132}Xe	^{126}Xe/^{132}Xe	^{127}Xe/^{132}Xe	^{128}Xe/^{132}Xe	^{129}Xe/^{132}Xe	^{130}Xe/^{132}Xe	^{131}Xe/^{132}Xe	^{134}Xe/^{132}Xe	^{136}Xe/^{132}Xe
38	0.085	12.0	—	not measurable	29.0	0.038 ± 0.002	0.075 ± 0.003	—	0.195 ± 0.002	1.357 ± 0.016	0.243 ± 0.004	1.55 ± 0.03	0.278 ± 0.008	0.244 ± 0.002
75	0.150	240.0	0.56	0.40 ± 0.06	25.0	0.0092 ± 0.0006	0.221 ± 0.002	0.436 ± 0.032	0.761 ± 0.008	3.77 ± 0.05	0.875 ± 0.023	54.97 ± 0.69	0.099 ± 0.003	0.077 ± 0.002
100	0.158	110.0	0.43	4.0 ± 0.6	20.7	0.0182 ± 0.0060	0.289 ± 0.004	0.555 ± 0.019	1.663 ± 0.018	3.887 ± 0.026	1.232 ± 0.012	19.49 ± 0.11	0.044 ± 0.001	0.021 ± 0.001
110	0.071	302.0	—	9.6 ± 1.3	20.3	0.0293 ± 0.0004	0.322 ± 0.003	0.615 ± 0.007	1.765 ± 0.017	3.510 ± 0.023	1.166 ± 0.009	12.41 ± 0.04	0.029 ± 0.001	⩽ 0.0039
120	0.069	294.0	—	20.3 ± 2.4	20.0	0.0650 ± 0.0007	0.385 ± 0.004	0.832 ± 0.014	2.029 ± 0.014	3.313 ± 0.015	0.995 ± 0.009	10.48 ± 0.04	0.028 ± 0.002	⩽ 0.0038
130	0.050	235.0	—	34.2 ± 4.1	19.5	0.0966 ± 0.0017	0.511 ± 0.004	1.164 ± 0.014	2.253 ± 0.011	3.484 ± 0.022	0.985 ± 0.009	8.78 ± 0.05	0.029 ± 0.001	⩽ 0.0051
140	0.096	206.0	—	39.3 ± 4.7	19.5	0.159 ± 0.002	0.857 ± 0.009	1.465 ± 0.029	2.326 ± 0.018	4.159 ± 0.032	1.061 ± 0.011	7.08 ± 0.04	0.027 ± 0.001	⩽ 0.0043
150	0.291	32.2	0.55	38.0 ± 5.2	19.5	0.223 ± 0.003	1.093 ± 0.026	1.600 ± 0.041	3.092 ± 0.027	4.253 ± 0.031	1.141 ± 0.007	6.663 ± 0.101	0.038 ± 0.001	0.014 ± 0.001
200	0.227	6.1	0.67	56.2 ± 7.3	18.8	0.285 ± 0.003	0.693 ± 0.010	1.053 ± 0.054	1.314 ± 0.011	2.004 ± 0.010	0.616 ± 0.006	2.259 ± 0.021	0.271 ± 0.005	0.217 ± 0.002
300	0.267	8.1	0.72	57.4 ± 7.4	15.0	0.344 ± 0.004	0.600 ± 0.009	0.714 ± 0.044	0.874 ± 0.009	1.489 ± 0.013	0.503 ± 0.006	1.571 ± 0.018	0.306 ± 0.003	0.241 ± 0.003
400	0.215	12.0	0.75	53.0 ± 7.9	17.2	0.840 ± 0.016	1.263 ± 0.016	1.337 ± 0.071	1.533 ± 0.017	1.807 ± 0.015	0.810 ± 0.004	2.069 ± 0.015	0.217 ± 0.003	0.158 ± 0.003
500	0.216	14.8	0.73	51.4 ± 7.7	18.4	0.641 ± 0.005	0.969 ± 0.007	1.037 ± 0.041	1.150 ± 0.009	1.603 ± 0.011	0.673 ± 0.009	1.859 ± 0.019	0.258 ± 0.004	0.185 ± 0.002
600	0.192	5.9	0.80	53.2 ± 6.9	18.0	0.427 ± 0.008	0.626 ± 0.006	0.664 ± 0.039	0.758 ± 0.009	1.337 ± 0.013	0.507 ± 0.008	1.338 ± 0.016	0.328 ± 0.005	0.262 ± 0.004

cross sections are based upon the ^{127}Xe cross sections and the mass spectrometrically determined $^{127}Xe/^{126}Xe$ ratios. In addition, the measurement of Funk *et al.* (1967) at 730 MeV and a measurement of a $BaCl_2$ sample at 600 MeV from our thick target experiment (Kaiser *et al.* 1975*a*, *b*) which in contrast was kept under vacuum in a quartz container during the proton-exposure are included. Table 4 lists the amounts of mass spectrometrically determined ^{136}Xe measured in the samples as well as in different blanks. The fluctuations of the proton-fluxes observed, especially in case of the Orsay samples, are due to the attempts to reduce the proton-beam-intensity.

As already discussed in the experimental section, two serious problems: 'thermal heating' during proton-exposure and 'leaching out' of Xe during preparation for the mass spectrometric analyses complicated the investigations. 'Thermal heating' during the proton-irradiation could have affected the proton-induced isotopic Xe yields depending upon the fraction of the Xe isotopes produced during proton-bombardment. Consequently, incorrect cross sections

TABLE 3

	proton-induced xenon									
energy / MeV	$^{124}Xe/^{126}Xe$	^{126}Xe / mbarn	$^{127}Xe/^{126}Xe$	$^{128}Xe/^{126}Xe$	$^{129}Xe/^{126}Xe$	$^{130}Xe/^{126}Xe$	$^{131}Xe/^{126}Xe$	$^{132}Xe/^{126}Xe$	$^{134}Xe/^{126}Xe$	$^{136}Xe/^{126}Xe$
38[a]	/	not measurable†	/	2.08 ± 0.10	8.70 ± 0.64	1.78 ± 0.09	13.80‡ ± 0.33	3.83 ± 0.52	0.03 ± 0.02	≡0
75[b]	0.038 ± 0.003	0.20 ± 0.03	1.980 ± 0.146	3.380 ± 0.048	16.10 ± 0.27	3.812 ± 0.110	248.8 ± 3.9	3.477 ± 0.031	0.036 ± 0.015	≡0
100[b]	0.062 ± 0.002	2.1 ± 0.3	1.922 ± 0.071	5.743 ± 0.101	13.21 ± 0.21	4.233 ± 0.072	67.32 ± 1.01	3.244 ± 0.058	0.067 ± 0.014	≡0
110[a]	0.094 ± 0.002	5.0 ± 0.6	1.913 ± 0.014	5.501 ± 0.041	10.93 ± 0.06	3.630 ± 0.038	38.59 ± 0.26	3.109 ± 0.025	0.091 ± 0.002	≤0.012
120[a]	0.169 ± 0.004	9.4 ± 1.2	2.163 ± 0.013	5.277 ± 0.044	8.616 ± 0.044	2.612 ± 0.015	27.25 ± 0.09	2.601 ± 0.010	0.073 ± 0.011	≤0.010
130[a]	0.189 ± 0.002	15.0 ± 1.8	2.277 ± 0.017	4.406 ± 0.021	6.814 ± 0.051	1.926 ± 0.016	17.17 ± 0.08	1.956 ± 0.016	0.056 ± 0.001	≤0.010
140[a]	0.186 ± 0.003	23.1 ± 2.8	1.710 ± 0.041	2.714 ± 0.034	4.854 ± 0.054	1.238 ± 0.016	8.268 ± 0.115	1.167 ± 0.019	0.032 ± 0.001	≤0.005
150[b]	0.213 ± 0.006	25.8 ± 3.7	1.464 ± 0.051	2.826 ± 0.072	3.855 ± 0.097	1.038 ± 0.026	6.06 ± 0.17	0.878 ± 0.026	0.020 ± 0.005	≡0
200[c]	0.410 ± 0.007	37.2 ± 5.3	1.524 ± 0.081	1.834 ± 0.031	1.965 ± 0.048	0.747 ± 0.014	2.52 ± 0.04	0.495 ± 0.033	0.023 ± 0.012	≡0
300[c]	0.571 ± 0.011	48.0 ± 6.8	1.195 ± 0.076	1.375 ± 0.026	1.289 ± 0.029	0.656 ± 0.014	1.66 ± 0.04	0.451 ± 0.007	0.037 ± 0.005	≡0
400[c]	0.665 ± 0.015	51.4 ± 7.6	1.060 ± 0.058	1.188 ± 0.021	1.059 ± 0.031	0.585 ± 0.008	1.34 ± 0.02	0.413 ± 0.023	0.025 ± 0.008	≡0
500[c]	0.661 ± 0.007	48.4 ± 7.4	1.072 ± 0.043	1.147 ± 0.013	1.087 ± 0.013	0.608 ± 0.011	1.28 ± 0.01	0.454 ± 0.005	0.042 ± 0.002	≡0
600[c]	0.679 ± 0.015	50.2 ± 7.1	1.064 ± 0.064	1.123 ± 0.020	0.905 ± 0.035	0.619 ± 0.015	1.14 ± 0.04	0.327 ± 0.021	0.032 ± 0.013	≡0
600[d]	0.721 ± 0.002			1.110 ± 0.001	1.103 ± 0.001	0.667 ± 0.002	1.152 ± 0.002	0.519 ± 0.001	0.0412 ± 0.0002	0.00506 ± 0.00008
730[e]	0.72 ± 0.02	43.0 ± 10.0	1.02 ± 0.02	1.14 ± 0.03	1.12 ± 0.02	0.72 ± 0.02	1.31 ± 0.03	0.55 ± 0.03	0.049 ± 0.003	

† The ^{126}Xe measurement was affected by air contamination due to the fact that the emission sensitivity had to be increased considerably.

‡ The cross section values are therefore based upon the ^{131}Xe yield; after correction for air contamination the (Xe-131) was estimated to be 3.0 mbarn [proton-flux = 12.0×10^{12} p/s].

[a] Orsay $BaCl_2$ samples (quartz encapsuled). [b] Orsay $BaCl_2$ samples (not quartz encapsuled).

[c] CERN $BaCl_2$ samples (not quartz encapsuled). [d] Thick target – 600 MeV $BaCl_2$ sample (quartz encapsuled).

[e] Funk *et al.* (1967) – 730 MeV $BaCl_2$ sample (encapsuled).

would have resulted. The fraction of the directly produced Xe varies from isotope to isotope (see table 1). However, it does not vary much with energy. For example, the fraction of ^{127}Xe produced during proton-exposure for 5 min is around 5 % for all energies where the experiments were executed. It turned out that ^{131}Xe would have been best suited for determining the cross sections since less than 0.1 % was produced during the respective irradiations. However,

TABLE 4. ^{136}Xe-CONCENTRATIONS IN THE SAMPLES INVESTIGATED AND IN THE RESPECTIVE BLANKS

sample / MeV	[^{136}Xe] in 10^{-12} cm^3 s.t.p./gBa	sample / MeV	[^{136}Xe] in 10^{-12} cm^3 s.t.p./gBa	blank	[^{136}Xe] in 10^{-12} cm^3 s.t.p./gBa
38	40.2 ± 4.4	150	24.0 ± 1.8	average of 3 hot blanks; $BaCl_2$	32.0 ± 8
75	37.0 ± 1.0	200	46.0 ± 0.4	compound in quartz finger;	
100	47.3 ± 2.2	300	88.1 ± 1.1	executed in the same procedure as the not encapsuled samples	
110	95.0	400	38.0 ± 0.8	average of 3 hot blanks; $BaCl_2$	0.18 ± 0.03
120	135.0	500	73.0 ± 0.8	compound quartz encapsulated (thick target)	
130	175.0	600	50.0 ± 1.8	average of 3 hot blanks; $BaCl_2$	0.20 ± 0.06
140	120.0	600†	111.0 ± 1.8	compound quartz encapsulated	
		125	68.0 ± 3.3	(thin target)	

† Thick target sample (Kaiser *et al.* 1975*a*, *b*).

due to the 'leaching' we had to rely upon the ^{127}Xe activity measurements. The maximum error due to 'thermal heating' is thus smaller than 5 % for this nuclide. In case of the CERN samples there are reasons to assume that isotopic changes due to 'thermal heating' can be neglected. The samples were exposed for a relatively short time (2 min) to a rather low proton-flux (the highest effective proton-flux at CERN was 1.48×10^{12} p/s at 500 MeV), thus resulting in relatively moderate heating. The excitation functions of the different Xe isotopes are impressively smooth in that energy range even for isotopes like ^{124}Xe, ^{126}Xe and ^{134}Xe which are almost entirely produced during the short time while the experiment was being performed (figures 3 and 4). The excitation function of the calibration reaction ^{27}Al (p, 3p3n) ^{22}Na, taken from Tobailem *et al.* (1966), is also included in figure 3. The transition of our values to the 730 MeV values obtained by Funk *et al.* (1967) is very smooth supporting our arguments that 'thermal heating' can be neglected in case of the CERN samples. A diffusive loss of ^{127}Xe can also be regarded as very small because the γ-counting was performed only 2 days after the respective irradiations. The mass spectrometric measurements were executed 4 months after the irradiations. Due to the process of 'leaching' described in the experimental section a considerable fraction of the xenon was driven out together with the water during preheating for the mass spectrometric analyses. By that time all the isobars had completely decayed to the respective Xe isotopes, so that no isotopic variations due to the 'leaching' occurred. The fraction of diffusive loss of Xe for the CERN samples ranged from 0.67 to 0.80 (table 2). This high degree of leaching represented an additional unanticipated complication in the evaluation of the data. Due to the experimental conditions the expected amounts of proton-induced Xe, especially for the heavy Xe isotopes, were already small and the process of 'leaching' caused the amounts to be reduced even further. In table 4 the amounts of ^{136}Xe measured in the various samples as well as in cold and hot blanks are listed. It is impossible to give estimates of the proton-induced ^{136}Xe yields in the non-encapsulated CERN and Orsay samples. In the thick target experiment mentioned

(Kaiser *et al.* 1975*a*, *b*) the preparation of the $BaCl_2$ samples was quite different. They were enclosed in quartz containers with breakable seals and kept under vacuum (10^{-4} Pa) during the irradiation. The central front sample of the thick target arrangement receiving the highest proton-dose and predominantly primary 600 MeV protons is included in table 3. The amount of ^{136}Xe found in that sample is about 600 times higher than the respective blank measurements (table 4). Based upon this data it can be concluded that there is a proton-induced ^{136}Xe contribution at 600 MeV. It proved to be fortunate for the evaluation of the 'thin target' data that the proton-induced ^{136}Xe yield is quite low. Evidently, the proton-induced ^{136}Xe yield could be considered to be zero.

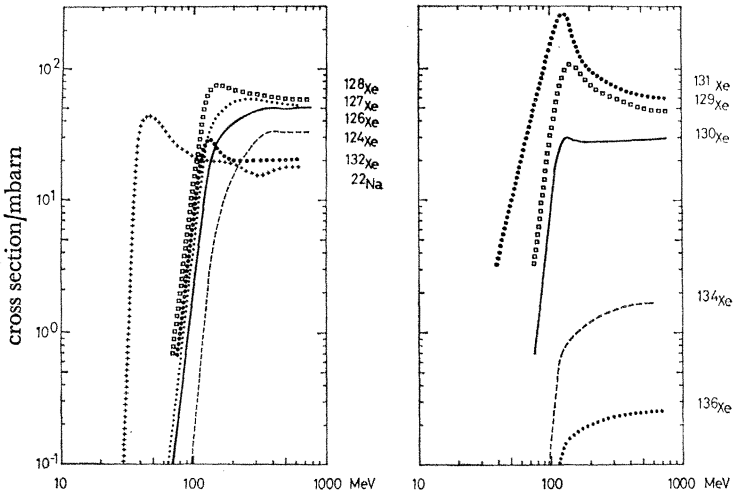

FIGURE 3. The graph displays the shapes of the excitation functions of the reactions Ba (p, X) ^{M}Xe. It contains the measurements of this study and the one of Funk *et al.* (1967) at 730 MeV. In order to make the diagram clearer it is divided into two parts. Scales are the same in both parts.

The Orsay irradiations containing samples which were not encapsulated were done some time after the CERN experiments. Based upon the experiences obtained earlier we used slightly modified target holders from the beginning. However, outgassing effects of the $BaCl_2$ compound when hit by the proton-beam caused vacuum problems of the synchro-cyclotron. It turned out that the effective proton-flux was on the average more than an order of magnitude higher than in case of the CERN irradiations. In addition, the energy loss of the protons within the targets increases with decreasing energy (Williamson *et al.* 1966). A combination of these effects led to a higher degree of 'thermal heating', thus enhancing the possibility of erroneous results. The storage time of the Orsay samples was shorter and the effect of 'leaching' was therefore smaller. It ranged from 0.43 to 0.56 (table 2). The proton-induced Xe spectra were obtained by assuming that the proton-induced ^{136}Xe yield was zero. However, due to the higher proton-dose received by the Orsay samples, the assumption that all the ^{136}Xe was air contamination does not essentially alter the Xe spectra, in contrast to the CERN samples. Although most of those Orsay measurements are already disregarded, they are mentioned here since diagrams showing excitation functions based upon these investigations have already been published (Kaiser *et al.* 1974*a*, *b*). These measurements were partly affected by 'thermal heating' leading to incorrect profiles for most of the excitation functions in the energy range up to 150 MeV. We repeated these measurements by scanning this energy range in very small steps

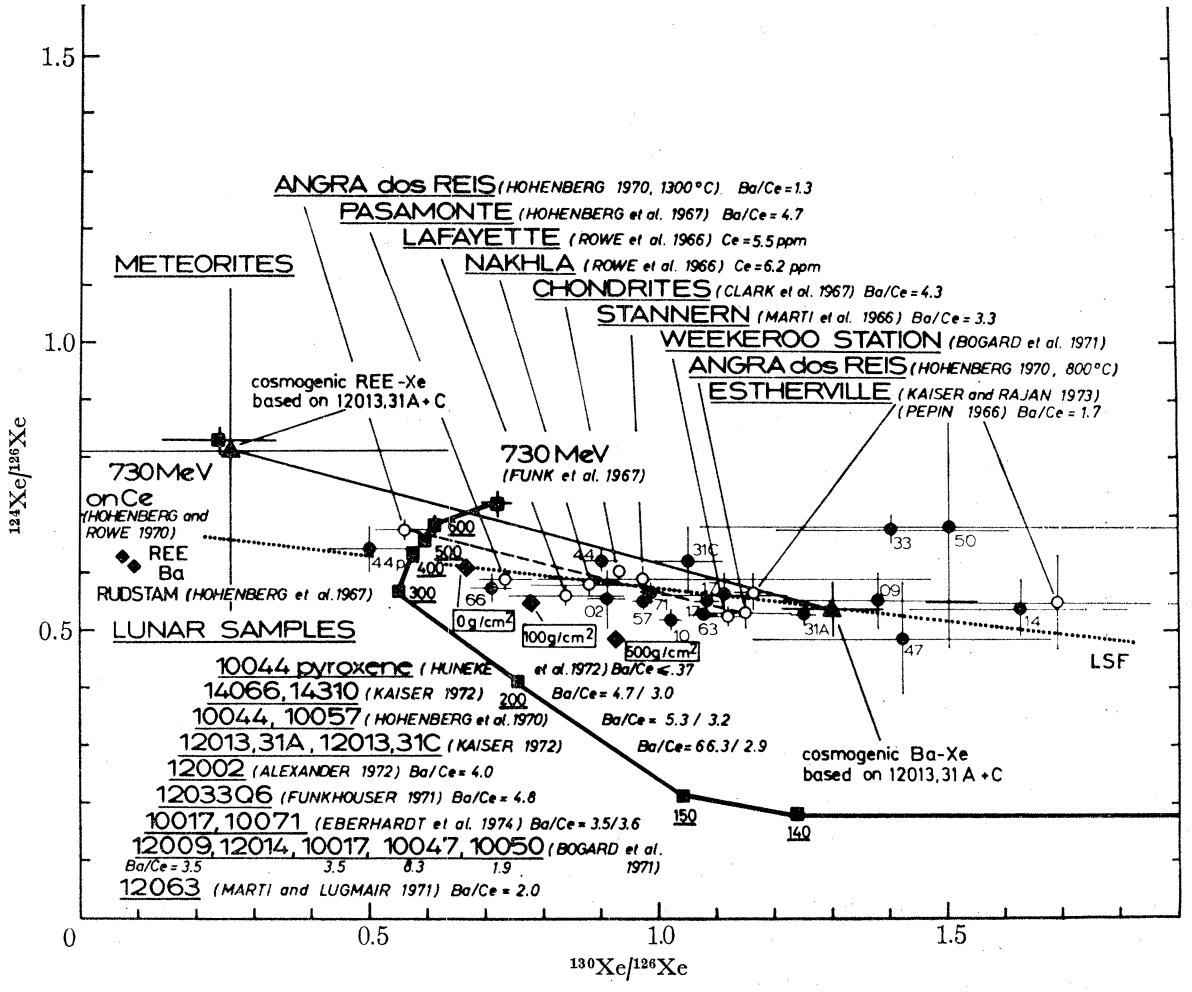

FIGURE 4. A correlation plot of purely cosmogenic, i.e. the 'trapped' ^{124}Xe, ^{126}Xe, and ^{130}Xe contributions are already subtracted, and proton-induced ^{124}Xe/^{126}Xe ratios against the respective ^{130}Xe/^{126}Xe ratios. Open circles represent meteoritic samples the names of which are included in the graph. Closed circles refer to the lunar samples. The numbers written on them are their last two digits of the lunar catalogue numbers. If available, the Ba/Ce ratios are given (for literature see table 6). The squares refer to target measurements. The points marked 140 to 730 represent the Xe ratios of proton-induced reactions on Ba targets. The numbers correspond to the excitation-energy in MeV. In addition, a measurement with protons of 730 MeV on Ce targets is included. The dotted line is a least squares fit (l.s.f.) through the meteoritic and lunar samples employing York's (1960) l.s.f. method. The solid line connecting the triangles represents the trend of the cosmogenic ^{124}Xe/^{126}Xe and ^{130}Xe/^{126}Xe ratios due to the different target chemistry (Ba-r.e.e.-system). Their values are based upon Xe measurements in the mineral separates of lunar breccia 12013. The dashed line connects the respective Xe ratios based upon the achondrite ANGRA dos REIS. The cosmogenic Xe ratios measured in the 800 °C fraction are mainly due to Ba targets whereas the cosmogenic Xe of the 1300 °C fraction is predominantly produced from r.e.e. targets. The diamonds marked Ba and REE in the left hand side of the graph display the Xe ratios obtained using the Rudstam formula. The diamonds marked 0 g/cm², 100 g/cm², and 500 g/cm² represent Xe ratios calculated using the proton-induced excitation functions on Ba and the depth dependent g.c.r.-fluxes of Reedy & Arnold (1972). They reflect the change of the Xe ratios with depth for proton-induced reactions on Ba.

(10 MeV). These measurements, with $BaCl_2$ samples in small quartz containers, showed that indeed considerable diffusive losses of, especially, the light isotopes (the expected abundances of the heavier isotopes concerned is anyway low) had occurred.

Discussion

The goal of this investigation was to use the thin target data in conjunction with the depth dependent galactic-cosmic-ray (g.c.r.) fluxes given by Reedy & Arnold (1972) for the lunar surface to obtain the isotopic composition of the cosmogenic Xe component as a function of depth.

In order to achieve this, the significance of four cosmogenic Xe contributions (not covered by the data presented here) has to be discussed and their consequent effects need to be considered properly.

(1) The Xe contributions from Ba targets with protons of energies smaller than 38 MeV and higher than 730 MeV (the highest proton-energy for which experimentally determined cross section values exist; Funk *et al.* (1967)).

(2) The Xe contributions from nuclear reactions of the type Ba (n, X) ^{M}Xe in the energy range from several MeV to around 80 to 100 MeV.

(3) The Xe contributions from rare earth element (r.e.e.) targets.

(4) The ^{130}Ba (n, γ) contribution to ^{131}Xe from low energy neutrons.

We discuss the above mentioned points in chronological order.

(1) The profiles of the excitation functions of all Xe isotopes investigated drop off towards lower proton-energies. This is obvious for all Xe products. It is thus justified to assume a monotonic decrease of the cross section curves for energies smaller than 38 MeV. For proton-energies greater than 730 MeV we rely essentially upon semi-empirically found evidence that the excitation functions of proton-induced nuclear reactions for higher than 730 MeV energies do not show major deviations from the values determined in this energy range. Estimates of the cross sections for proton-energies above 730 MeV utilizing the Rudstam formula IDED-G (Rudstam 1966) also yielded similar profiles. However, the cross sections thus obtained level off at somewhat higher absolute values than those obtained by simple extrapolation of the measured ones. The experimentally determined excitation functions attain constant values around 300 Me whereas in case of the theoretically calculated ones the corresponding energy range is around 1 GeV. Since the essential energy range in which nuclear structure governs the cross section variations is covered experimentally, it appears justified to use the cross section values

Table 5

	'total' production per atom Ba per second [$\times 10^{-27}$]			production ($\lesssim$ 730 MeV) per atom Ba per second [$\times 10^{-27}$]		
isotope	0 g/cm^2	200 g/cm^2	500 g/cm^2	0 g/cm^2	200 g/cm^2	500 g/cm^2
^{124}Xe	79.5	21.6	2.0	52.8	18.3	1.77
^{126}Xe	133.8	42.3	4.26	93.4	37.3	3.9
^{128}Xe	179.8	70.7	7.9	134.4	65.0	7.5
^{129}Xe	178.2	82.7	9.9	141.0	77.8	9.6
^{130}Xe	91.1	34.9	3.9	66.8	31.9	3.7
^{131}Xe	275.9	167.1	22.5	229.7	161.2	22.1
^{132}Xe	62.9	25.5	2.9	46.8	23.5	2.8
^{134}Xe	4.6	1.4	0.14	3.1	1.2	0.13
^{136}Xe	0.60	0.19	0.02	0.41	0.16	0.02

resulting by simply extrapolating the 730 MeV measurements to higher proton-energies and assuming that the cross section curves remain constant as shown in figure 3. Minor deviations from constancy have only insignificant effects on the production rates ($P(^{M}Xe) \sim \phi(\text{g.c.r.}) \times \sigma(^{M}Xe)$) since the depth dependent galactic-cosmic-ray fluxes, ϕ(g.c.r.), drop off steeply for proton-energies above 600 MeV (roughly with a power law $E^{-2.5}$). Estimates of the fractions of the various Xe isotopes produced up to the proton-energy of 730 MeV are given in table 5.

(2) Above a certain energy (around 80–100 MeV) the excitation functions of proton and neutron induced nuclear reactions behave similarly. However, below that energy, differences in the shapes of the excitation functions should be expected due to the existence of the Coulomb potential. No experimentally determined Ba(n, X)^{M}Xe cross sections as functions of energy for any of the following reactions are available so far.

(1) ^{130}Ba (n, 2n) . . . ^{129}Xe
(2) ^{132}Ba (n, α) ^{129}Xe
(3) ^{130}Ba (n, 3n) . . . ^{128}Xe
(4) ^{130}Ba (n, p) . . . ^{130}Xe
(5) ^{132}Ba (n, p) . . . ^{132}Xe
(6) ^{135}Ba (n, α) ^{132}Xe
(7) ^{132}Ba (n, 2n) . . . ^{131}Xe
(8) ^{134}Ba (n, α) ^{131}Xe
(9) ^{137}Ba (n, α) ^{134}Xe

Cross section values for some of the reactions exist in literature for neutrons with a fission energy spectral distribution (for relevant references see CINDA (1972)). There exist also experimental cross section data as well as theoretical cross section estimates for some of these reactions for the neutron-energy of 14 MeV (Qaim 1975). As already mentioned by Hohenberg *et al.* (1967) the reactions ^{130}Ba (n, p) . . . ^{130}Xe and ^{132}Ba (n, p) . . . ^{132}Xe seem to contribute measurable portions to the cosmogenic ^{130}Xe and ^{132}Xe yields. These processes will be particularly operative at greater depths where the ratio of effective neutrons to protons increases.

(3) We plot in figure 4 purely cosmogenic (proton-induced) ^{124}Xe/^{126}Xe against cosmogenic (proton-induced) ^{130}Xe/^{126}Xe. The Ba/Ce ratios are given in table 6 (Ce is representative of the r.e.e.). Two facts are obvious from a study of this plot. The purely cosmogenic Xe ratios display a linear distribution whereby high ^{124}Xe/^{126}Xe ratios correspond to low ^{130}Xe/^{126}Xe ratios and vice versa. Further, the distribution is not correlated with the Ba/Ce ratio. These observations hold good for meteoritic samples as well as for lunar samples. From the studies on the achondrite Angra dos Reis by Hohenberg (1970) and on the lunar breccia 12013 by Kaiser (1971) it is known in which part of this graph the cosmogenic ^{124}Xe/^{126}Xe and the ^{130}Xe/^{126}Xe ratios from r.e.e. targets are located. Nevertheless, samples like 14066 with a Ba/Ce ratio of 4.7 (table 6) are found far to the left and Estherville with a Ba/Ce ratio of 1.7 (table 6) far to the right, thus exhibiting just the opposite of what would be expected if the chemistry is mainly responsible for this distribution. In course of these investigations samples of a mineral enriched in r.e.e. were irradiated and mass spectrometric analyses will be carried out in the near future. Due to the complexity of the γ-spectra of those samples no reliable ^{127}Xe and ^{131}Ba activity measurements could be obtained. So for the moment, statements about the effectiveness of a contribution of cosmogenic Xe produced from r.e.e. targets are mainly based upon information from literature (Hohenberg *et al.* 1967; Hohenberg & Rowe 1970; Hohenberg 1970; Kaiser 1971; Burnett *et al.* 1971; Bogard *et al.* 1971; Huneke *et al.* 1972; Lugmair & Marti 1972; Srinivasan 1974; Reedy

1975). It seems, however, that in samples with a Ba/Ce ratio $\geqslant 2$ (e.g. Estherville, Kaiser & Rajan 1973) the cosmogenic Xe due to Ba targets predominates the isotopic composition of the observed cosmogenic Xe spectra.

TABLE 6. CONCENTRATIONS OF Ba AND Ce IN THE METEORITES AND LUNAR SAMPLES USED IN GRAPH 4

sample	Ba (parts/10^6)	Ce (parts/10^6)	reference
Angra dos Reis	26.4[a]	20.6[a]	[a] Schnetzler & Philpotts (1969)
Pasamonte	38.0[b]	8.1[c]	[b] Gast (1965)
Lafayette	—	5.5[d]	[c] Schmitt *et al.* (1963)
Nakhla	—	6.2[d]	[d] Schmitt *et al.* (1964)
ave. Chondrites	4[e]	0.94[c]	[e] Schnetzler (1971)
Stannern	42.2[f]	12.9[d]	[f] Wyttenbach & Dulakas (1966) in Marti *et al.* (1966)
Estherville	5[g]	3.0[c]	[g] Duke & Silver (1967)
10044 pyroxene	8.9[h]	$\leqslant 24$[i]	[h] Huneke *et al.* (1972)
14066	840[j]	180[j]	[i] Goles *et al.* (1970)
14310	610[k]	207[k]	[j] Laul *et al.* (1972)
10044	234[l]	44[l]	[k] Taylor *et al.* (1972)
10057	280[m]	88[m]	[l] Wänke *et al.* (1970)
12013,31A	6360[n]	96[n]	[m] Morrison *et al.* (1970)
12013,31C	1112[n, o]	380[n]	[n] Schnetzler *et al.* (1971)†
12002	67[p]	17[p]	[o] Wakita & Schmitt (1971)†
12033	723[p]	151[p]	[p] Hubbard *et al.* (1971)
10017	270[q]	77.3[i]	[q] Eberhardt *et al.* (1974)
10071	298[q]	83[r]	[r] Gast *et al.* (1970)
12009	60[s]	17[t]	[s] Compston *et al.* (1971)
10047	250[u]	~30‡[u]	[t] Haskin *et al.* (1971)
10050	70[u]	37[u]	[u] Wakita *et al.* (1971)
12063	60[v]	30[v]	[v] Taylor *et al.* (1971)
	140[w]	19[w]	[w] Wänke *et al.* (1971)

† See Kaiser (1971).
‡ Estimated from the La content Wakita *et al.* (1971).

(4) The situation is somewhat different in case of the ^{130}Ba(n, γ) contribution. The first rare gas measurements of lunar samples revealed the existence of an enhancement of this isotope in cosmogenic Xe (e.g. Hohenberg *et al.* 1970; Marti *et al.* 1970; Pepin *et al.* 1970). Investigations by Kaiser (1972), Kaiser & Berman (1972), Eberhardt *et al.* (1974), and Kaiser & Rajan (1973) led to the result that the enrichment of the cosmogenic ^{131}Xe yield is correlated with Ba and that the average resonance integral of the reaction ^{130}Ba(n, γ) is *ca.* 200 barn. It was thus sufficiently high to explain plausibly the enrichment observed, especially after establishing that the enhancement was correlated with high ^{158}Gd/^{157}Gd ratios (Eugster *et al.* 1970; Marti & Lugmair 1971), indicators of low energy neutron fluxes. Berman & Browne (1973) determined the resonance energies and the necessary line-width parameters of that reaction so that the 'effective' resonance integral (Dresner 1956) could be obtained.

The depth dependent low energy neutron fluxes in the lunar regolith were calculated by Lingenfelter *et al.* (1972). Recently, the depth dependent low energy neutron fluxes were experimentally determined by Burnett *et al.* (1975) in their l.n.p.e. (lunar neutron probe experiment) (Woolum *et al.* 1973; Woolum & Burnett 1974*a*, *b*). Burnett & Russ (1975) developed procedures allowing to infer from the data available the depth dependent production rate of ^{131}Xe produced via the reaction ^{130}Ba (n, γ).

Thus, in contrary to the 3 points discussed above the Xe contribution due to the ^{130}Ba (n, γ) reaction is known and the depth dependent ^{131}Xe yield composed of the Ba(p, X)...^{131}Xe and the ^{130}Ba (n, γ)...^{131}Xe contributions can be obtained.

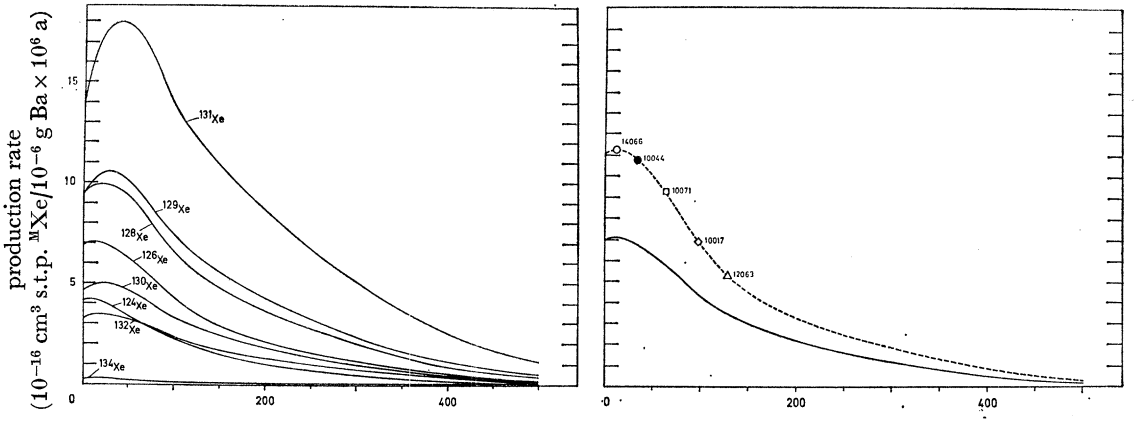

FIGURE 5 FIGURE 6

FIGURE 5. The graph displays the 'estimated' production rates of proton-induced Xe isotopes on Ba targets for the depth range from 0 g/cm² to 500 g/cm² in the lunar regolith. They were estimated using the proton-induced excitation functions (see text) and the depth dependent g.c.r.-fluxes of Reedy & Arnold (1972).

FIGURE 6. The solid curve is the 'estimated' production rate of proton-induced ^{126}Xe on Ba. This curve is already included in figure 5. Its 'surface' (0 g/cm²) production rate is 7.0×10^{-16} cm³ s.t.p. ^{126}Xe/10^{-6} g Ba × 10^6 a. The open circle represents lunar sample 14066, a lunar sample for which the cosmic-ray irradiation history is simple (see text), and which thus allows to infer with a relatively high degree of certainty a real cosmogenic 'surface' (2π geometry) production rate of ^{126}Xe. Its value is 11.3×10^{-16} cm³ s.t.p. ^{126}Xe/10^{-6} g Ba × 10^6 a. The dashed curve is obtained by multiplying the 'estimated' production rates with the factor of 1.6 which is the difference of the truly cosmogenic 'surface' production rate of ^{126}Xe in 14066 compared to the respective 'estimated' one. The symbols representing lunar samples 10044, 10071, 10017, and 12063 are fitted on this curve at the respective depths estimated on the basis of their cosmogenic Xe ratios (figure 7). The thus derived sample individual production rates of ^{126}Xe are used for estimating the exposure ages based upon the amount of cosmogenic ^{126}Xe from Ba targets (table 8) in those samples.

APPLICATION TO ACTUAL LUNAR SAMPLES

The production rates $P(^{M}Xe) = \sigma\phi NT$ [10^{-16} cm³ s.t.p. ^{M}Xe/10^{-6} g Ba × 10^6 a] of the diverse stable Xe isotopes as functions of depth were obtained using the proton-induced excitation functions determined in this study, the cross section values at 730 MeV measured by Funk *et al.* (1967), the extrapolated cross section curves (see point 1), and the depth dependent g.c.r. fluxes of Reedy & Arnold (1972) for depths from 0 to 500 g/cm² in the lunar regolith. The curves are displayed in figure 5. They are marked by a steady increase to maximum values between 10 and 50 g/cm² depths followed by exponential decreases. Figure 6 shows separately the production rate of ^{126}Xe thus obtained. It includes, in addition, the cosmogenic production rate measured in lunar breccia 14066 (Srinivasan 1974). The reason for including the lunar samples 10044, 10071, 10017, and 12063 will be given later.

Breccia 14066 is an interesting case. The cosmogenic ^{131}Xe/^{126}Xe ratio found is the lowest one measured till now in a lunar sample (Kaiser 1972; Srinivasan 1974) (^{131}Xe/^{126}Xe = 2.75 ± 0.22; Srinivasan 1974). The ^{81}Kr–^{83}Kr exposure age is $27.8 \pm 0.5 \times 10^6$ a (Srinivasan 1974), an age which is concordant with the Cone Crater event. Its burial as well as its irradiation history is

rather simple. The breccia was buried in a shielded location and got ejected at the time the Cone Crater was formed. The ^{81}Kr–^{83}Kr exposure age defines in this case the 'real' exposure age, i.e. the averaged galactic-cosmic-ray and solar-cosmic-ray flux, ϕ(g.c.r. + s.c.r.), was the same for ^{81}Kr and ^{83}Kr during the total exposure. Enhancement of the ^{81}Kr production relative to the ^{83}Kr production due to a relatively short irradiation ('suntan' age, Lal 1974) late in the exposure history did not take place in 14066. Effects of this kind are discussed by Marti & Lugmair (1971) for lunar sample 12002 and by Eberhardt *et al.* (1974) for lunar rock 10017. The Ba/Ce ratio of 14066 is 4.7 (table 6). The cosmogenic Xe, the most abundant component in the xenon of 14066, is therefore predominantly from Ba targets.

A certain complication arose in trying to extract the cosmogenic Xe composition because of the fact that 14066 contains some 'parentless', i.e. not *in situ* produced fissiogenic Xe from the spontaneous decay of ^{244}Pu. This made it somewhat more difficult to estimate the amount of the 'trapped' Xe component. The most abundant Xe isotope in fissiogenic Xe is ^{136}Xe which has an almost negligible yield in cosmogenic Xe. The measured concentration of ^{136}Xe consists therefore mainly of fissiogenic and 'trapped' Xe. An uncertainty in the estimation of the fissiogenic Xe contribution consequently affects the determination of the 'trapped' Xe concentration. In case of the lunar samples, normally the 'trapped' Xe is determined assuming that all the ^{136}Xe which can not be explained as *in situ* produced fissiogenic Xe from the spontaneous decay of ^{238}U as being 'trapped' Xe. The isotopic composition of the 'trapped' Xe component may lie somewhere between Xe of 'solar wind' composition and Xe of 'terrestrial atmosphere' composition. This leads to the result that the cosmogenic yields of those isotopes abundant in 'trapped' Xe (^{129}Xe, ^{131}Xe, ^{132}Xe and ^{134}Xe) are often affected by large uncertainties. The amount of cosmogenic ^{126}Xe due to Ba targets was obtained utilizing the formula given by Srinivasan (1974) (table 7) resulting in a production rate of 11.3×10^{-16} cm^3 s.t.p. ^{126}Xe/10^{-6} g Ba $\times 10^6$ a for 14066. The figure obtained using the proton-induced excitation function of ^{126}Xe and the depth dependent g.c.r. fluxes of Reedy & Arnold (1972) is 7.0×10^{-16} cm^3 s.t.p. ^{126}Xe/10^{-6} g Ba $\times 10^6$ a. The difference is not really striking considering the uncertainties of the parameters involved: the absolute values of the depth dependent g.c.r. fluxes, the absolute values of the cross sections, the Xe amounts due to high energy neutron-induced reactions, production from r.e.e. targets, and to some extent the Ba concentration and true irradiation geometry of 14066. The more serious uncertainties seem to be associated with the 'estimated' production rate of ^{126}Xe. Therefore, the measured cosmogenic ^{126}Xe production rate of breccia 14066 is taken as the 'surface' production rate of ^{126}Xe. So the depth dependent cosmogenic ^{126}Xe production rate was obtained by normalizing the proton-induced ^{126}Xe-curve to that 'surface' (14066) value. The depth dependent Xe production rates allow the proton-induced Xe ratios to be determined as function of depth. These ratios are independent of the absolute cosmogenic ^{126}Xe production rate used. They are displayed in figure 7. The essential feature of this graph is that besides the ^{131}Xe/^{126}Xe ratio some of the other proton-induced Xe ratios quite considerably increase with depth, thus, for example, the proton-induced ^{128}Xe/^{126}Xe ratio varies from 1.3 to 1.85 in the depth range given, and the proton-induced ^{129}Xe/^{126}Xe ratio varies from 1.4 to 2.35. This offers the possibility to use these ratios as depth indicators, too.

In case of the lunar samples the use of the cosmogenic ^{129}Xe/^{126}Xe ratio which displays the largest but one variation with depth as depth indicator involves two problems:

(1) The difficulty of estimating the 'trapped' ^{129}Xe contribution. This is often complicated by the fact that the 'trapped' Xe component is a mixture of 'solar wind' Xe and 'terrestrial

TABLE 7

sample	$^{81-83}$Kr age [Ma]	$^{126}Xe_{cosm.}$(T)† $^{126}Xe_{cosm.}$(Ba) [$\times 10^{-12}$ cm^3 s.t.p./g]	Ba	La	Ce (parts/10^6)	Pr	U	depth g/cm^2	crys. age [Ga]	^{126}Xe-exposure age [Ma]	suntan age [Ma]	n-flux(^{158}Gd/^{157}Gd) $^{81-83}$Kr exp. age	^{126}Xe exp. age cm^{-2} s^{-1}
14066	27.8[a] ± 0.5	32.2 ± 2.1[a] 26.4 ± 1.7	840[b]	76[b]	180[b]	—	4.0[b]	10	—	27.8 ± 0.5	27.8 ± 0.5	—	—
10044	70[c] ± 17	12.6 ± 0.85[g] 11.0 ± 0.74	234[a]	12[a]	44[a]	—	0.28[a]	35	—	41 ± 4	—	⩽ 0.26[g]	⩽ 0.46[g]
10071	350[f] ± 15	140[f] ± 30 112 ± 24	298[f]	29[g]	83[g]	—	0.86[h]	70	2.88 ± 0.06[f]	430 ± 100	—	0.39[g] + 0.04	0.32[g] ± 0.08
12063	95[i] ± 5	3.3 ± 0.4[i]	60[j]	9.8[j]	30[j]	4.2[j]	0.15[j]	145	2.65 ± 0.12[i]	117 ± 20	2.8[k]	1.56[i] ± 0.10	1.28[i] ± 0.28
10017	480[f] ± 25	160 ± 30[f]	270[f]	26.6[g]	77.3[g]	12.9[l]	0.86[h]	85	2.35 ± 0.06[f]	600 ± 125	4.2[k]	1.15[g] ± 0.07	0.92[g] ± 0.20

[a] Srinivasan (1974); [b] Laul *et al.* (1972); [c] Hohenberg *et al.* (1970); [d] Wänke *et al.* (1970); [e] Eugster *et al.* (1970); [f] Eberhardt *et al.* (1974); [g] Gast *et al.* (1970); [h] Tatsumoto (1970); [i] Marti & Lugmair (1970); [j] Taylor *et al.* (1971); [k] Lal (1975 private communication); [l] Wakita & Schmitt (1970).

† $^{126}Xe_{cosm.}$ (Ba) = ((1.20 ± 0.09) × (g Ba/g)/(1.20 ± 0.09) × (g Ba/g) + (0.73 ± 0.05) × (gr.e.e./g)) × $^{126}Xe_{cosm.}$(T), where r.e.e. = La + Pr + Ce.

atmosphere' Xe (the respective yields are quite distinct: $(^{129}Xe/^{136}Xe)_{s.w.} = 3.60 \pm 0.06$, Kaiser (1972); $(^{129}Xe/^{136}Xe)_{air} = 2.98 \pm 0.02$, Nier (1950)) and that some of the lunar samples contain 'parentless' fissiogenic Xe (e.g. 14066, Srinivasan (1974)).

(2) The eventual contribution of ^{129}Xe due to the reactions $^{130}Ba(n, 2n)\ldots{}^{129}Xe$ and $^{132}Ba(n, \alpha)^{129}Xe$. Their excitation functions are not known yet. There exists, however, experimental evidence (Qaim 1975, private communication) that the cross section of the (n, 2n) reaction predominates, at least at 14 MeV, over all other (n, charged particle) reactions, especially with respect to the (n, α) reaction.

The problem of using the cosmogenic $^{129}Xe/^{126}Xe$ ratio as depth indicator is particularly important in meteorites due to the contribution of radiogenic ^{129}Xe from the decay of now extinct ^{129}I.

In case of the proton-induced $^{128}Xe/^{126}Xe$ ratio the problems just discussed are less significant. The abundance of ^{128}Xe in 'trapped' Xe is low ($(^{128}Xe/^{136}Xe)_{s.w.} = 0.289 \pm 0.031$, Kaiser (1972); $(^{128}Xe/^{136}Xe)_{air} = 0.216 \pm 0.001$, Nier (1950)). Relatively wide variations in the amount and in the isotopic composition of the 'trapped' Xe have only minor effects on the cosmogenic ^{128}Xe yield. The excitation function of the reaction $^{130}Ba(n, 3n)\ldots{}^{128}Xe$ is also unknown but is expected to yield much lower cross section values than those for $^{130}Ba(n, 2n)\ldots{}^{129}Xe$ (Qaim 1975). Another problem in this case is a contribution of neutron-capture produced ^{128}Xe via the reaction $^{127}I(n, \gamma)^{128}Xe$ with low energy neutrons. Iodine is usually correlated with the other halogenes, like, for example, bromine. The measurement of the Kr then provides a clue whether an enhancement of the ^{128}Xe yield due to the neutron-capture reaction on ^{127}I can be expected since low energy neutron reactions on ^{79}Br and ^{81}Br cause enhancements of the cosmogenic ^{80}Kr and ^{82}Kr yields (Marti *et al.* 1969) the ratio of which is $(^{80}Kr/^{82}Kr)_{nc} = 2.69 \pm 0.28$ (14310, Lugmair & Marti 1972).

Figure 7 and table 8 contain some selected samples for which the cosmogenic Xe yields are well determined and the cosmogenic $^{131}Xe/^{126}Xe$ ratios are different. They are used to demonstrate the applicability of the results obtained and to indicate also its limitations. In order not to complicate the graph, only 5 characteristic samples (but 7 data sets) are included. The cosmogenic $^{131}Xe/^{126}Xe$ ratio varies from 2.75 (14066, Srinivasan (1974)) to 7.6 (12063, Marti & Lugmair (1971)). Intermediate $^{131}Xe/^{126}Xe$ ratios are displayed by 10044 (Hohenberg *et al.* (1970), $(^{131}Xe/^{126}Xe)_{cosm.} = 3.85$), 10071 (Eberhardt *et al.* (1974), $(^{131}Xe/^{126}Xe)_{cosm.} = 5.3$; Bogard *et al.* (1971) $(^{131}Xe/^{126}Xe)_{cosm.} = 5.2$). The reason for including lunar rock 10017 (Eberhardt *et al.* (1974) $(^{131}Xe/^{126}Xe)_{cosm.} = 7.87$; Marti *et al.* (1970) $(^{131}Xe/^{126}Xe)_{cosm.} = 7.92$) will be given later.

All samples have Ba/Ce ratios > 2. As is evident, the cosmogenic Xe is thus predominantly from Ba targets. The essential conclusions deducible from figures 7 and 8 are given below:

(1) The proton-induced $^{128}Xe/^{126}Xe$ as well as the proton-induced $^{129}Xe/^{126}Xe$ ratios define in almost all measurements displayed the same burial depths. Exceptions are the measurements of Eberhardt *et al.* (1974) for lunar rock 10017 and 10071. Since this observation is likely to lead to some speculations it will be discussed in more detail. Both rocks are extensively studied (Eberhardt *et al.* 1974; Marti *et al.* 1970; Bogard *et al.* 1972). Thus, several Xe measurements are available and they exhibit relatively wide variations in the cosmogenic $^{129}Xe/^{126}Xe$ ratio (table 8). Of especial interest is the cosmogenic Xe spectrum derived by Eberhardt *et al.* (1974) for 10017. The cosmogenic $^{129}Xe/^{126}Xe$ ratio is 1.49 ± 0.06 and is thus lower than the cosmogenic $^{128}Xe/^{126}Xe$ ratio of 1.57 ± 0.03. This is hard to understand since the proton-induced

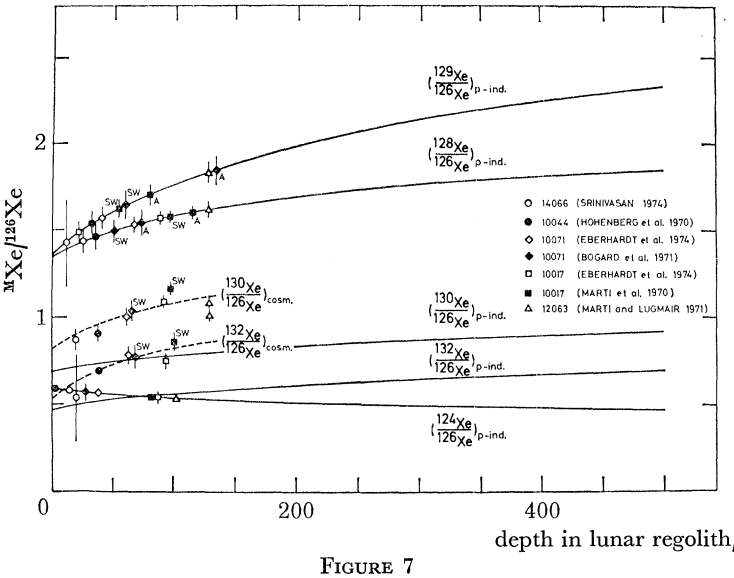

FIGURE 7

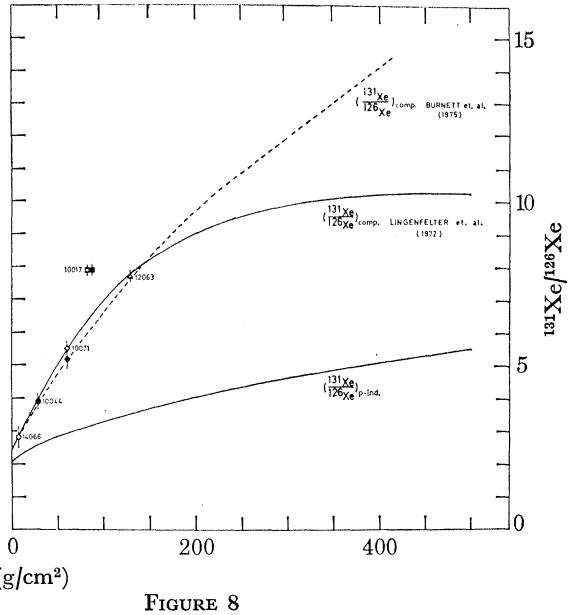

FIGURE 8

depth in lunar regolith/(g/cm^2)

FIGURE 7. The graph displays the proton-induced ^{M}Xe/^{126}Xe ratio (M = 124, 128, 129, 130, and 132) as a function of depth in the lunar regolith (solid curves). The shapes of the curves were obtained by dividing values of the depth dependent production rate curves of the diverse Xe isotopes by the respective ones of ^{126}Xe. They are independent of the choice of the absolute production rate of ^{126}Xe. The symbols representing the lunar samples listed were placed on that part of the respective curves to which the measured cosmogenic Xe ratios corresponded. In this way, burial depth estimates based upon individual cosmogenic Xe ratios were obtained (for ^{M}Xe/^{126}Xe ratios; M = 124, 128, and 129). In essence, the curves for M = 128 and 129 can be used for estimating the burial depths since their variation with depth is large enough. In case of the lunar samples 14066, 10044, and 12063 both proton-induced Xe ratios indicate essentially the same burial depths demonstrating the validity of the conclusion drawn that the proton-induced isotopic Xe ratios on Ba can be associated with the cosmogenic ones on Ba in those cases (see text). In case of the lunar rocks 10017 and 10071 (cosmogenic Xe determinations of Eberhardt *et al.* 1974) there is a disagreement in the burial depth estimates based on those Xe ratios. Therefore, cosmogenic Xe compositions of these particular rocks deduced from the Xe measurements of Marti *et al.* (1970) and Bogard *et al.* (1971), respectively, are included. The cosmogenic Xe ratios were obtained assuming that the ^{136}Xe yield is composed of an *in situ* produced fissiogenic Xe contribution due to the spontaneous decay of ^{238}U and a 'trapped' Xe contribution (A corresponds to a 'trapped' contribution of 'terrestrial atmosphere' composition; SW corresponds to a 'trapped' contribution of 'solar wind' composition). The cosmogenic ^{130}Xe/^{126}Xe and ^{132}Xe/^{126}Xe ratios were in almost all cases too high to fit the respective proton-induced ^{130}Xe/^{126}Xe and ^{132}Xe/^{126}Xe curves anywhere in the depth range given (see text). Therefore, their measured cosmogenic Xe ratios were placed at the depth positions determined by the ^{128}Xe/^{126}Xe and ^{129}Xe/^{126}Xe ratios. The cosmogenic shapes of these two Xe ratios were then estimated by fitting curves through the data points (dashed curves).

FIGURE 8. The proton-induced ^{131}Xe/^{126}Xe ratio as a function of depth is given. In addition, the shape of the 'composed' ^{131}Xe/^{126}Xe ratio is included utilizing the ratio of the depth dependent production rates of the 'estimated' ^{131}Xe and ^{126}Xe yields (figure 5), the depth dependent absolute production rate of ^{126}Xe based upon lunar breccia 14066 (figure 6), and the depth dependent neutron-capture produced ^{131}Xe contribution due to the ^{130}Ba(n, γ) reaction in the lunar regolith (the derivation of it is given in the text). The dashed curve is the one obtained using the depth dependent ^{131}Xe production rates of the reaction ^{130}Ba(n, γ) of Burnett *et al.* (1975) and the depth dependent absolute proton-induced ^{126}Xe and ^{131}Xe production rates (see text). The measured cosmogenic ^{131}Xe/^{126}Xe ratios of the 5 lunar samples used for demonstration are placed at the depth positions estimated on the basis of their cosmogenic ^{128}Xe/^{126}Xe and ^{129}Xe/^{126}Xe ratios. The good agreement in 4 cases for both curves evidences that the 'composed' ^{131}Xe/^{126}Xe ratio coincides quite well with the cosmogenic ^{131}Xe/^{126}Xe ratio from Ba targets. The explanation of the displacement of the point representing the measurement of lunar rock 10017 is given in the text.

PHILOSOPHICAL TRANSACTIONS OF THE ROYAL SOCIETY A MATHEMATICAL, PHYSICAL & ENGINEERING SCIENCES

TABLE 8. COSMOGENIC Xe SPECTRA OF THE LUNAR SAMPLES USED FOR DEMONSTRATION

sample	$\frac{^{124}Xe}{^{126}Xe}$	$\frac{^{128}Xe}{^{126}Xe}$	$\frac{^{129}Xe}{^{126}Xe}$	$\frac{^{130}Xe}{^{126}Xe}$	$\frac{^{131}Xe}{^{126}Xe}$	$\frac{^{132}Xe}{^{126}Xe}$	$\frac{^{134}Xe}{^{126}Xe}$	remarks
14066[a]	0.577 ± 0.020	1.479 ± 0.054	1.42 ± 0.25	0.864 ± 0.050	2.75 ± 0.22	0.54 ± 0.25	—	—
10044[b]	0.62 ± 0.02	1.47 ± 0.09	1.55 ± 0.06	0.90 ± 0.03	3.87 ± 0.12	0.70 ± 0.02	0.04 ± 0.01	—
10071[c]	0.564 ± 0.017	1.530 ± 0.029	1.540 ± 0.065	1.005 ± 0.016	5.49 ± 0.13	0.780 ± 0.045	0.067 ± 0.022	—
[d]	0.58 ± 0.04	1.47 ± 0.07	1.62 ± 0.10	1.04 ± 0.05	5.12 ± 0.23	0.76 ± 0.07	0.06 ± 0.02	'trapped' Xe = solar wind
[d]	0.58 ± 0.04	1.53 ± 0.07	1.84 ± 0.09	1.08 ± 0.05	5.26 ± 0.23	0.89 ± 0.07	0.08 ± 0.02	'trapped' Xe = air
10017[c]	0.548 ± 0.013	1.570 ± 0.028	1.490 ± 0.055	1.077 ± 0.017	7.87 ± 0.12	0.785 ± 0.05	0.074 ± 0.022	
[e]	0.548 ± 0.006	1.58 ± 0.02	1.61 ± 0.05	1.17 ± 0.01	7.92 ± 0.08	0.87 ± 0.05	0.092 ± 0.017	'trapped' Xe = solar wind
[e]	0.550 ± 0.006	1.60 ± 0.02	1.70 ± 0.05	1.11 ± 0.01	7.98 ± 0.07	0.92 ± 0.04	0.10 ± 0.02	'trapped' Xe = air
[d]	0.55 ± 0.02	1.53 ± 0.05	1.27 ± 0.08	1.02 ± 0.03	7.50 ± 0.18	0.53 ± 0.06	0.04 ± 0.03	'trapped' Xe = solar wind
[d]	0.55 ± 0.03	1.58 ± 0.04	1.73 ± 0.05	1.10 ± 0.03	7.70 ± 0.18	0.81 ± 0.03	0.088 ± 0.016	'trapped' Xe = air
12063[f]	0.54 ± 0.01	1.60 ± 0.03	1.82 ± 0.05	1.07 ± 0.03	7.65 ± 0.12	1.01 ± 0.04	0.075 ± 0.014	'trapped' Xe = solar wind
[f]	0.54 ± 0.01	1.61 ± 0.03	1.88 ± 0.05	1.08 ± 0.02	7.69 ± 0.13	1.04 ± 0.03	0.082 ± 0.013	'trapped' Xe = air

[a] Srinivasan (1974); [b] Hohenberg *et al.* (1970); [c] Eberhardt *et al.* (1974); [d] Bogard *et al.* (1971); [e] Marti *et al.* (1970); [f] Marti & Lugmair (1971).

$^{129}Xe/^{126}Xe$ ratio from Ba targets are always greater than the proton-induced $^{128}Xe/^{126}Xe$ ratios (figure 7) for all depths. The scanty data of cosmogenic Xe from r.e.e. targets also indicate a higher yield for cosmogenic ^{129}Xe than for ^{128}Xe (Hohenberg & Rowe 1970; Hohenberg 1970; Kaiser 1971; Huneke *et al.* 1972). The corresponding cosmogenic $^{129}Xe/^{126}Xe$ ratios deduced from the measurement of Marti *et al.* (1970) (table 8) are 1.61 ± 0.05 assuming a 'trapped' Xe contribution of 'solar wind' composition which normally should be present in lunar samples and a value of 1.70 ± 0.05 assuming a 'trapped' Xe contribution of 'terrestrial atmosphere' composition. Both values are higher than the one derived by Eberhardt *et al.* (1974) and are easily explainable with proton-induced Xe from Ba targets. The cosmogenic $^{129}Xe/^{126}Xe$ ratios deduced from the measurement of Bogard *et al.* (1971) are 1.27 ± 0.08 ('trapped' Xe of 'solar wind' composition) and 1.73 ± 0.05 ('trapped' Xe of 'terrestrial atmosphere' composition). All data sets are corrected for *in situ* produced fissiogenic Xe from the spontaneous decay of ^{238}U (fissiogenic Xe yields are from Wetherill (1953); for crystallization ages and U concentrations see table 7). The measurement of Marti *et al.* (1970) is independent of the choice of the 'trapped' Xe contribution. It leads to reasonable values of cosmogenic $^{129}Xe/^{126}Xe$ ratios. The cosmogenic $^{128}Xe/^{126}Xe$ ratios are practically unaffected by the choice of the 'trapped' Xe composition and are in good agreement in the three data sets. By comparing the different Xe measurements it appears that the specimen of 10017 measured by Marti *et al.* (1970) contains the lowest amounts of ^{136}Xe whereas the sample investigated by Bogard

et al. (1971) contained the highest amounts. The correction for 'trapped' Xe was thus smallest in the sample of Marti *et al.* (1970). The cosmogenic Xe spectrum derived from that measurement (table 8) seems to be close to the true value. The cosmogenic Xe spectrum derived by Eberhardt *et al.* (1974) and the one deduced from the measurement of Bogard *et al.* (1971) under the assumption that 'trapped' Xe is similar to 'solar wind' composition on the other hand leads to some difficulties. It seems rather improbable that the 'trapped' Xe in the basaltic rock 10017 is mostly due to contamination with terrestrial Xe. It is also unlikely that a contamination of this amount originating from the extraction system can be found in labs of the quality of Berne (Eberhardt *et al.* 1974) or Houston (Bogard *et al.* 1971). But considerable portions of the 'trapped' Xe had to be of terrestrial composition to bring the cosmogenic ^{129}Xe/^{126}Xe ratio in the range set by the measurement of Marti *et al.* (1970). Therefore, we propose two possible solutions.

(*a*) Rock 10017 contained originally a 'trapped' Xe contribution similar to the 'terrestrial atmosphere' composition as recently found in some lunar samples (Lightner & Marti 1974; Leich & Niemeyer 1975; Bogard & Gibson 1975).

(*b*) Rock 10017 contained some 'parentless' fissiogenic xenon besides a 'trapped' Xe contribution of 'solar wind' composition.

We like to favour the second suggestion. In essence, the statements made for 10017 are valid for 10071, too (table 8). In continuation, we feel that other Apollo 11 rocks may also contain 'parentless' fissiogenic Xe, e.g. 10057 (Hohenberg *et al.* 1970; the cosmogenic ^{129}Xe/^{126}Xe ratio derived there is 1.00 ± 0.07 whereas the cosmogenic ^{128}Xe/^{126}Xe ratio is 1.58 ± 0.08).

In summary, the good agreement of the derived burial depths using the cosmogenic ^{128}Xe/^{126}Xe and ^{129}Xe/^{126}Xe ratios indicates that the (n, 2n) and (n, α) reactions on ^{130}Ba and ^{132}Ba do not contribute essentially to the cosmogenic ^{128}Xe and ^{129}Xe yields. That does not mean that the cross sections of the ^{130}Ba(n, 2n)...^{129}Xe and ^{132}(n, α)^{129}Xe reactions are small. On the contrary, the cross section values at 14.5 MeV for the ^{130}Ba(n, 2n)...^{129}Cs* reaction is 1370 ± 70 mbarn (Bormann *et al.* 1974). Probably, there is a partial contribution of ^{129}Cs* via the reaction ^{130}Ba(n, pn)^{129}Cs* but despite this, the ^{130}Ba(n, 2n) cross section at 14.5 MeV is expected to be around 1000 mbarn (Qaim 1975). In addition, the position of the maximum for the excitation function of this reaction is in the vicinity of that energy (Qaim 1975). From the maximum value the cross section gradually decreases towards higher neutron-energies. Following the systematics of (n, α) reactions at 14–15 MeV the cross section of the reaction ^{132}Ba(n, α)^{129}Xe (asymmetry parameter $(N-Z)/A = 0.151$) is around 10 mbarn and it is not expected to exceed this value significantly at any other neutron-energy (Qaim 1975). As an example, the cross section of the (n, α) reaction on ^{138}Ba at 14.5 MeV is 2.0 ± 0.02 mbarn (Bormann *et al.* 1974). The low abundance of ^{130}Ba and ^{132}Ba in natural barium, 0.101 % and 0.097 %, respectively, and the fact that the depth dependent high energy neutron fluxes (10 MeV to 100 MeV) are orders of magnitudes lower (Armstrong & Alsmiller 1971; Lingenfelter *et al.* 1972) than the respective proton-fluxes (Reedy & Arnold 1972) clearly indicate that the neutron-induced contributions are insignificant. Thus, the depth dependent behaviour of the cosmogenic ^{128}Xe/^{126}Xe and ^{129}Xe/^{126}Xe ratios is explainable with proton-induced reactions on Ba targets. In case the cosmogenic ^{128}Xe and ^{129}Xe yields can accurately be determined the cosmogenic ^{128}Xe/^{126}Xe and the ^{129}Xe/^{126}Xe ratios serve as ideal depth indicators since their variations with depth is rather large and they seem to be unaffected by fast (< 30 MeV) and slow (thermal and epithermal) neutron reactions.

PHILOSOPHICAL TRANSACTIONS OF THE ROYAL SOCIETY A MATHEMATICAL, PHYSICAL & ENGINEERING SCIENCES

(2) The cosmogenic $^{130}Xe/^{126}Xe$ ratios are higher than the respective proton-induced $^{130}Xe/^{126}Xe$ ratios. That implies that the contribution of ^{130}Xe via the reaction $^{130}Ba(n, p)^{130}Xe$ can not be neglected. From the systematics of the cross sections of the (n, 2n), (n, p) and (n, α) reactions (Qaim 1975; Bormann *et al.* 1974) it follows that the (n, p) cross sections at 14–15 MeV are much lower than the respective (n, 2n) cross sections. There exists a measurement of the cross section of the (n, p) reaction on ^{136}Ba by Bormann *et al.* (1974) at 14.5 MeV having a value of 49 ± 10 mbarn thus supporting the systematics. However, following empirical rules the (n, p) cross section at 14–15 MeV is expected to increase by a factor of about 1.5 if the mass of the target nucleus is reduced by one mass unit (1 neutron). This would lead to a cross section of *ca.* 550 mbarn for the $^{130}Ba(n, p)\ldots^{130}Xe$ reaction. Since the position of the maximum of the (n, p) excitation function is presumably around 25 MeV (Qaim 1975, private communication) the maximum cross section will be higher thus falling in the range of the (n, 2n) cross sections. Such a high cross section value is however only possible for the neutron-deficient isotopes of barium. In conjunction with the fact that the proton-induced cross section for the reaction $Ba(p, X)\ldots^{129}Xe$ is higher than the corresponding one leading to ^{130}Xe this may explain why the (n, p) produced contribution is significant in cosmogenic ^{130}Xe whereas the (n, 2n) produced ^{129}Xe is not. Since the burial depths of the samples used for demonstration are determined by the cosmogenic $^{128}Xe/^{126}Xe$ and $^{129}Xe/^{126}Xe$ ratios, the depth dependent cosmogenic $^{130}Xe/^{126}Xe$ ratios can be estimated (dashed curve in figure 7).

(3) The cosmogenic $^{134}Xe/^{126}Xe$ ratio (although the measured values in table 8 show large error bars) seems to be well explainable with proton-induced reactions on barium. The (n, α) reaction on ^{137}Ba (most but one abundant isotope in natural barium = 11.32 %) does thus not contribute significantly to the cosmogenic ^{134}Xe yield (see point 1, too).

(4) The depth dependent cosmogenic $^{132}Xe/^{126}Xe$ ratio seems also to be underestimated by the proton-induced $^{132}Xe/^{126}Xe$ ratio. The contribution of ^{132}Xe via the reactions $^{132}Ba(n, p)\ldots^{132}Xe$ and $^{135}Ba(n, \alpha)^{132}Xe$ has to be considered. The explanation of the depth dependency of the cosmogenic $^{134}Xe/^{126}Xe$ ratio with proton-induced reactions on Ba indicates that the (n, p) reaction seems to be playing some role.

(5) The proton-induced $^{131}Xe/^{126}Xe$ ratio increases drastically from 2.1 to 5.6 in the depth range given (figure 8) demonstrating the importance of the low energy-proton-induced ^{131}Xe contribution.

(6) The 'composed' $^{131}Xe/^{126}Xe$ ratio (i.e. inclusion of the neutron-capture produced contribution of ^{131}Xe due to $^{130}Ba(n, \gamma)$ (Kaiser & Berman 1972; Eberhardt *et al.* 1971) varies in the same range from 2.4–$\sim$15. The depth dependency of the 'composed' $^{131}Xe/^{126}Xe$ ratio was estimated in two ways.

(*a*) The 'effective' resonance integral of the reaction $^{130}Ba(n, \gamma)$ was determined utilizing the resonance parameters measured by Berman & Browne (1972) and the method of Nordheim (1961) and was calculated with the computer program ZUT of Teuchert (1968). The depth dependent low energy neutron-fluxes were taken from Lingenfelter *et al.* (1972) and the absolute depth dependent proton-induced ^{131}Xe and ^{126}Xe contributions were obtained using the excitation functions measured in this study, the depth dependent g.c.r.-fluxes of Reedy & Arnold (1972), and the 'surface' production rate of $^{126}Xe(Ba)$ measured in 14066.

(7) The cosmogenic $^{131}Xe/^{126}Xe$ ratios yield in 4 cases surprisingly similar burial depths as deduced from the cosmogenic $^{128}Xe/^{126}Xe$ and $^{129}Xe/^{126}Xe$ ratios. This suggests that the (n, 2n) reaction on ^{132}Ba and the (n, α) reaction on ^{134}Ba do not add essentially to the cosmogenic

^{131}Xe yield (see points 1 and 2, too). The cosmogenic ^{131}Xe/^{126}Xe ratio of 10017 is clearly above the cosmogenic ^{131}Xe/^{126}Xe curve (figure 8). This sample received by far the highest low energy neutron-dose of all lunar samples determined by Gd measurements till now (Eugster *et al.* 1970; ^{158}Gd/^{157}Gd $= 1.59879 \pm 0.00040 \mathrel{\widehat{=}} \psi_{th} = 17.4 \pm 0.06 \times 10^{15}$ n/cm^2). The derived neutron-flux assuming the ^{81}Kr–^{83}Kr exposure age given by Eberhardt *et al.* (1974) of $480 \pm 25 \times 10^6$ y to be correct, is $\phi_{th} = 1.15 \pm 0.07$ n/cm^2 s which is much higher than the one derived for 10071 (Eugster *et al.* 1970; ^{158}Gd/^{157}Gd $= 1.58970 \pm 0.00027 \mathrel{\widehat{=}} \psi_{th} = 4.3 \pm 0.4 \times 10^{15}$ n/cm^2; ^{81}Kr–^{83}Kr exposure age $= 350 \pm 15 \times 10^6$ a, Eberhardt *et al.* 1974) of $\phi_{th} = 0.39 \pm 0.04$ n/cm^2 s, although the exposure ages and the burial locations are quite similar (table 7, figure 8). The cosmogenic ^{131}Xe/^{126}Xe ratio of rock 10017 is too high for this depth. The most plausible explanation is a 3 stage irradiation history. Before the sample was transferred to 80 g/cm^2 depth it must have been buried in a previously shielded location where it built up the ^{158}Gd/^{157}Gd enhancement and a cosmogenic Xe component strongly enriched in ^{131}Xe due to neutron-capture on ^{130}Ba.

(8) The cosmogenic ^{128}Xe/^{126}Xe, ^{129}Xe/^{126}Xe and ^{131}Xe/^{126}Xe ratios indicate for lunar sample 12063 the same burial depth (140 g/cm^2) a result also obtained by Marti & Lugmair (1971) utilizing other physical reasons. This speaks for a simple irradiation history. Despite this fact the deduced low energy neutron-flux is very high compared to the one inferred from the calculations of Lingenfelter *et al.* (1972). Since the low energy neutron-dose measurement (by means of the ^{158}Gd/^{157}Gd ratio, Marti & Lugmair 1971) is correct, the difficulty seems to be related to the value of the exposure age. There are some suggestions indicating that the exposure age values are questionable. And that concerns the ^{81}Kr–^{83}Kr exposure age as well as the ^{126}Xe–Ba–r.e.e. exposure age. The 'suntan' age of this sample is 2.8×10^6 a (Lal 1975, private communication). Thus, the production rate of ^{81}Kr at this depth and at the top surface (0 g/cm^2) is at least a factor 2–3 different (based upon the ^{81}Kr excitation function of Sr(p, X)...^{81}Kr, measured in this lab and the depth dependent g.c.r.-fluxes of Reedy & Arnold (1972)). As far as the ^{126}Xe–Ba–r.e.e. exposure age is concerned, the total amount of cosmogenic ^{126}Xe measured by Bogard *et al.* (1971) in that sample is twice as much ($= 6.6 \times 10^{-12}$ cm^3 s.t.p. ^{126}Xe$_{cosm.}$/g) as was found by Marti & Lugmair (1971) (table 7). Judging from the measurements of Taylor *et al.* (1971) and Wänke *et al.* (1971) (table 6) the relevant trace element concentrations seem to be inhomogeneously distributed in 12063 and an uncertainty in the Ba and r.e.e. concentrations affects the ^{126}Xe–Ba–r.e.e. exposure age determination.

(9) From the agreement in burial depth locations utilizing the cosmogenic Xe ratios in the cases of 14066, 10044, 10071 and 12063 it can be concluded that they experienced essentially a two stage irradiation history.

Real' exposure ages can be obtained using the depth dependent production rate of one stable Xe isotope, preferably ^{126}Xe, since it is predominantly produced by high energy particles. The burial depth can be derived from the cosmogenic Xe ratios. The respective depth dependent ^{126}Xe production rate can be taken from figure 6. If the concentrations of cosmogenic ^{126}Xe, Ba, and the r.e.e. are known, the amount of cosmogenic ^{126}Xe from Ba targets, normalized to 10^{-6} g Ba, can be estimated utilizing the formula given by Srinivasan (1974) (table 7). The quotient of the amount of cosmogenic ^{126}Xe(Ba) and the depth dependent production rate is thus the exposure age in 10^6 a (table 7). The depth dependent ^{126}Xe production rates used for estimating the ^{126}Xe exposure ages are included in figure 6. We think that this method of exposure age determination represents the best approach in estimating the time a sample was exposed to cosmic-rays (c.r.). We, therefore, call it the 'real' exposure age. Processes limiting

the general use of the ^{81}Kr–^{83}Kr method (Marti & Lugmair 1971) play only a secondary role. The 'suntan' ages of most of the lunar samples are in the range of a few Ma (Lal 1974). This is relatively short compared to the 'real' exposure ages of those samples (table 7). It is, however, long compared to the half-life of the ^{81}Kr activity (2.1×10^5 a). It is sufficient to bring the ^{81}Kr activity in equilibrium with the higher particle flux ϕ(g.c.r. + s.c.r.) at the top surface and causing thus enhancements of the cosmogenic $^{81}Kr/^{83}Kr$ ratio (in rock 12002 almost a factor of 2, Marti & Lugmair 1971) which in turn lead to exposure ages underestimating the time the sample was exposed to cosmic-rays. Besides, ^{126}Xe is produced at high particle-energies ($E \geqslant 150$ MeV) scarcely found in s.c.r. (Lal 1974). Thus, the enhancement is essentially caused by the higher g.c.r. fluxes at the surface. For the samples discussed in this work the enhancement is negligible.

The author wants to thank Professor W. Herr, director of this institute, for supporting this work. The cooperative help of Dr P. Rösner in executing the computer calculations is gratefully appreciated. The author is indebted to Drs A. Herz (CERN, Genève) and Mrs G. Gerschel (Institut de Physique Nucléaire, Orsay) for their keen interest and readiness to furnish irradiation time. Especial thanks are addressed to Professor M. Barbier (CERN) for many fruitful discussions which the author considerably benefitted from Mr F. Hoffmann, Mr F. Schofel, and the operators of the 600 MeV synchro-cyclotron (CERN) are thanked for their spontaneously offered assistance in executing these experiments. The assistance of Dr W. Berg and the operators of the 152 MeV synchro-cyclotron (Orsay) in performing the even more subtle experiments there is gratefully acknowledged. Dr M. Heimann is thanked for taking some of the Al data. Professor D. Lal, Professor R. C. Reedy, Professor M. N. Rao and Dr M. S. Qaim are thanked for critical discussion of the results obtained. Finally, the author wants to express his gratefulness to the 'Deutsche Forschungsgemeinschaft' for granting a stipendium and supplying the travel expenses. The 'Bundesministerium für Forschung und Technologie' is thanked for financial support.

References (Kaiser)

Albee, A. L., Burnett, D. S., Chodos, A. A., Eugster, O. J., Huneke, J. C., Papanastassiou, D. A., Podosek, F. A. Russ, III, G. P., Sanz, H. G., Tera, F. & Wasserburg, G. J. 1970 *Science, N.Y.* **167**, 463.
Alexander, E. C., Jr. 1971 *Proc. 2nd Lunar Sci. Conf. Suppl.* 2, **2**, 1643.
Armstrong, T. W. & Alsmiller, R. G., Jr. 1971 *Proc. 2nd Lunar Sci. Conf. Suppl.* 2, **2**, 1729.
Arnold, J. R., Honda, M. & Lal, D. 1961 *J. geophys. Res.* **66**, 3519.
Berman, B. L. & Browne, J. C. 1973 *Phys. Rev.* C **7**, 2522.
Bogard, D. D., Funkhouser, J. G., Schaeffer, O. A. & Zähringer, J. 1971 *J. geophys. Res.* **76**, 2757.
Bogard, D. D., Huneke, J. C., Burnett, D. S. & Wasserburg, G. J. 1971 *Geochim. cosmochim. Acta* **35**, 1231.
Bogard, D. D. & Gibson, E. K. 1975 Abstract Volume 6*th Lunar Sci. Conf.* 63.
Bormann, M., Neuert, H. & Scobel, W. 1974 In *Handbook on nuclear activation cross sections*, Tech. Rep. Ser. 156. Vienna: IAEA.
Burnett, D. S., Huneke, J. C., Podosek, F. A., Price Russ, III, G. & Wasserburg, G. J. 1971 *Proc. 2nd Lunar Sci. Conf. Suppl.* 2, **2**, 1671.
Burnett, D. S., Drozd, R. J., Morgan, C. J. & Podosek, F. A. 1975 *Proc. 6th Lunar Sci. Conf. Suppl.* 6, **3**, 2219.
CINDA 72 1972 June *An index to the literature on microscopic data.* Vienna: IAEA.
Clark, R. S., Rao, M. N. & Kuroda, P. K. 1967 *J. geophys. Res.* **72**, 5143.
Compston, W., Berry, H., Vernon, M. J., Chappell, B. W. & Kaye, M. J. 1971 *Proc. 2nd Lunar Sci. Conf. Suppl.* 2, **2**, 1471.
Dresner, L. 1956 *Nucl. Sci. Engng* **1**, 68.
Duke, M. B. & Silver, L. T. 1967 *Geochim. cosmochim. Acta* **31**, 1637.
Eberhardt, P., Geiss, J. & Graf, H. 1971 *Earth Planet. Sci. Lett.* **12**, 260.

Eberhardt, P., Geiss, J., Graf, H., Grögler, N., Krähenbühl, U., Schwaller, H. & Stettler, A. 1974 *Geochim. cosmochim. Acta* **38**, 97.
Eugster, O., Tera, F., Burnett, D. S. & Wasserburg, G. J. 1970 *Earth Planet. Sci. Lett.* **8**, 20.
Funk, H., Podosek, F. & Rowe, M. W. 1967 *Earth Planet. Sci. Lett.* **3**, 193.
Funkhouser, J. 1971 *Earth Planet. Sci. Lett.* **12**, 263.
Gast, P. W. 1965 *Science, N.Y.* **147**, 858.
Gast, P. W., Hubbard, N. J. & Wiesmann, H. 1970 *Proc. 1st Lunar Sci. Conf. Suppl.* 1, **2**, 1143.
Goles, G. G. & Anders, E. 1961 *J. geophys. Res.* **66**, 889.
Goles, G. G., Randle, K., Osawa, M., Lindstrom, D. J., Jerome, D. Y., Steinborn, T. L., Beyer, R. L., Martin, M. R. & McKay, S. M. 1970 *Proc. 1st Lunar Sci. Conf. Suppl.* 1, **2**, 1177.
Haskin, L. A., Helmke, P. A., Allen, R. O., Anderson, M. R., Korotev, R. L. & Zweifel, K. A. 1971 *Proc. 2nd Lunar Sci. Conf. Suppl.* 2, **2**, 1307.
Hohenberg, C. M. 1970 *Geochim. cosmochim. Acta* **34**, 185.
Hohenberg, C. M., Davis, P. K., Kaiser, W. A., Lewis, R. S. & Reynolds, J. H. 1970 *Proc. 1st Lunar Sci. Conf. Suppl.* 1, **2**, 1283.
Hohenberg, C. M., Munk, M. N. & Reynolds, J. H. 1967 *J. geophys. Res.* **72**, 3139.
Hohenberg, C. M. & Rowe, M. W. 1970 *J. geophys. Res.* **75**, 4205.
Hubbard, N. J. & Gast, P. W. 1971 *Proc. 2nd Lunar Sci. Conf. Suppl.* 2, **2**, 999.
Huneke, J. C., Podosek, F. A., Burnett, D. S. & Wasserburg, G. J. 1972 *Geochim. cosmochim. Acta* **36**, 269.
Kaiser, W. A. 1971 *Proc. 2nd Lunar Sci. Conf. Suppl.* 2, **2**, 1627.
Kaiser, W. A. 1972*a* *Earth Planet. Sci. Lett.* **13**, 387.
Kaiser, W. A. 1972 Report Univ. Calif. Berkeley.
Kaiser, W. A. & Berman, B. L. 1972 *Earth Planet. Sci. Lett.* **15**, 320.
Kaiser, W. A., Damm, G., Herpers, U., Herr, W., Kulus, H., Michel, R., Rösner, K. P., Thiel, K. & Weigel, H. 1975 *Proc. 6th Lunar Sci. Conf. Suppl.* 6, **2**, 1927.
Kaiser, W. A. & Rajan, R. S. 1973 *Earth Planet. Sci. Lett.* **20**, 286.
Kaiser, W. A., Rösner, K. P. & Herr, W. 1974*a* *Meteoritics* **10**, 94.
Kaiser, W. A., Rösner, K. P. & Herr, W. 1974*b* Paper presented at the Conference: Interactions of the interplanetary plasma with the modern and ancient moon, Lake Geneva, Wisconsin, U.S.A. (ed. D. R. Criswell and J. W. Freeman).
Krummenacher, D., Merrihue, C. M., Pepin, R. O. & Reynolds, J. H. 1961 *Geochim. cosmochim. Acta* **26**, 231.
Lal, D. 1974 *Phil. Trans. R. Soc. Lond.* A **277**, 395.
Laul, J. C., Wakita, H., Showalter, D. L., Boynton, W. V. & Schmitt, R. A. 1972 *Proc. 3rd Lunar Sci. Conf. Suppl.* 3, **2**, 1181.
Lederer, C. M., Hollander, J. M. & Perlman, I. 1968 *Table of Isotopes* (6th ed.). New York: John Wiley.
Leich, D. A. & Niemeyer, S. 1975 *Abstract volume, 6th Lunar Sci. Conf.* 504.
Lightner, B. D. & Marti, K. 1974 *Proc. 5th Lunar Sci. Conf. Suppl.* 5, **2**, 2023.
Lingenfelter, R. E., Canfield, E. H. & Hampel, V. E. 1972 *Earth Planet. Sci. Lett.* **16**, 355.
Lugmair, G. W. & Marti, K. 1972 *Proc. 3rd Lunar Sci. Conf. Suppl.* 3, **2**, 1891.
Marti, K., Eberhardt, P. & Geiss, J. 1966 *Z. Naturf.* **21a**, 398.
Marti, K. & Lugmair, G. W. 1971 *Proc. 2nd Lunar Sci. Conf. Suppl.* 2, **2**, 1591.
Marti, Shedlovsky, J. P., Lindstrom, R. M., Arnold, J. R. & Bhandari, N. G. 1969 In *Meterorite Research* (ed. P. M. Millman).
Meixner, C. 1971 *Gammaenergien*, Jül.-811-RX.
Merrihue, C. 1966 *J. geophys. Res.* **71**, 263.
Morrison, G. H., Gerard, J. T., Kashuba, A. T., Gangadharam, E. V., Rothenberg, A. M., Potter, N. M. & Miller, G. B. 1970 *Proc. 1st Lunar Sci. Conf. Suppl.* 1, **2**, 1383.
Nier, O. A. 1950 *Phys. Rev.* **79**, 450.
Nordheim, L. W. 1961 General Atomic Report GA-2527.
Pepin, R. O. 1966 *J. geophys. Res.* **71**, 2815.
Pepin, R. O., Nyquist, L. E., Phinney, D. & Black, D. C. 1970 *Proc. 1st Lunar Sci. Conf. Suppl.* 1, **2**, 1435.
Qaim, S. M. 1975 Conference on Nuclear Cross Sections and Technology, Washington D.C. 3–7 March 1975.
Reedy, R. C. 1975 *Eos* **56**, 387.
Reedy, R. C. & Arnold, J. R. 1972 *J. geophys. Res.* **77**, 537.
Reynolds, J. H. 1960*a* *Phys. Rev. Lett.* **4**, 351.
Reynolds, J. H. 1960*b* *Z. Naturf.* **15a**, 1112.
Rowe, M. W. 1967 *Earth Planet. Sci. Lett.* **2**, 92.
Rowe, M. W. & Bogard, D. D. 1966 *J. geophys. Res.* **71**, 686.
Rowe, M. W. & Bogard, D. D. 1966 *J. geophys. Res.* **71**, 4183.
Rowe, M. W., Bogard, D. D. & Kuroda, P. K. 1966 *J. geophys. Res.* **71**, 4679.
Rowe, M. W., Bogard, D. D., Brothers, C. E. & Kuroda, P. K. 1965 *Phys. Rev. Lett.* **15**, 843.
Rudstam, G. 1966 *Z. Naturf.* **21a**, 1027.

PHILOSOPHICAL TRANSACTIONS OF THE ROYAL SOCIETY A MATHEMATICAL, PHYSICAL & ENGINEERING SCIENCES

Schmitt, R. A., Smith, R. H., Lasch, J. E., Mosen, A. W., Olehy, D. A. & Vasilevskis, J. 1963 *Geochim. cosmochim. Acta* **27**, 577.
Schmitt, R. A., Smith, R. H. & Olehy, D. A. 1964 *Geochim. cosmochim. Acta* **28**, 67.
Schnetzler, C. C. & Philpotts, J. A. 1969 *Proc. of a Symposium on Meteorite Research* (ed. P. M. Millman).
Schnetzler, C. C., Philpotts, J. A. & Bottino, M. L. 1970 *Earth Planet. Sci. Lett.* **9**, 185.
Schnetzler, C. C. 1971 *Meteorites* (ed. B. Mason). Gordon & Breach.
Shedlovsky, J. P., Honda, M., Reedy, R. C., Evans, J. C., Lal, D., Lindstrom, R. M., Delany, A. C., Arnold, J. R., Loosli, H. H., Fruchter, J. S. & Finkel, R. C. 1970 *Proc. 1st Lunar Sci. Conf. Suppl.* 1, **2**, 1503.
Srinivasan, B. 1974 *Proc. 5th Lunar Sci. Conf. Suppl.* 5, **2**, 2033.
Tatsumoto, M. 1970 *Proc. 1st Lunar Sci. Conf. Suppl.* 1, **2**, 1595.
Taylor, S. R., Rudowski, R., Muir, P., Graham, A. & Kaye, M. 1971 *Proc. 2nd Lunar Sci. Conf. Suppl.* 2, **2**, 1083.
Taylor, S. R., Kaye, M., Muir, P., Nance, W., Rudowski, R. & Ware, N. 1972 *Proc. 3rd Lunar Sci. Conf. Suppl.* 3, **2**, 1231.
Teuchert, E. 1968 *KFA Jülich Report* Jül-551-RG.
Tobailem, J., de Lassus St-Genies, C. H. & Leveque, L. 1971 Centre d'Études Nucléaires de Saclay, CEA-N-1466(1).
Wakita, H., Rey, P. & Schmitt, R. A. 1971 *Proc. 2nd Lunar Sci. Conf. Suppl.* 2, **2**, 1319.
Wakita, H. & Schmitt, R. A. 1970 *Earth Planet. Sci. Lett.* **9**, 164.
Wakita, H., Schmitt, R. A. & Rey, P. 1970 *Proc. 1st Lunar Sci. Lett. Suppl.* 1, **2**, 1685.
Wänke, H., Rieder, R., Baddenhausen, H., Spettel, B., Teschke, F., Quijano-Rico, M. & Balacescu, A. 1970 *Proc. 1st Lunar Sci. Conf. Suppl.* 1, **2**, 1719.
Wänke, H., Wlotzka, F., Baddenhausen, H., Balacescu, A., Spettel, B., Teschke, F., Jagoutz, E., Kruse, H., Quijano-Rico, M. & Rieder, R. 1971 *Proc. 2nd Lunar Sci. Conf. Suppl.* 2, **2**, 1187.
Wetherill, G. W. 1953 *Phys. Rev.* **92**, 907.
Williamson, C. F., Boujot, J.-P. & Picard, J. 1966 *Rapport CEA-R* 3042.
Woolum, D. S., Burnett, D. S. & Bauman, C. A. 1973 In *Abstract volume, 4th Lunar Science Conf.*, 793.
Woolum, D. S. & Burnett, D. S. 1974*a* *Earth Planet. Sci. Lett.* **21**, 153.
Woolum, D. S. & Burnett, D. S. 1974*b* In *Abstract volume, 5th Lunar Science Conf.*, 848.
York, D. 1966 *Can. J. Phys.* **44**, 1079.

PHILOSOPHICAL TRANSACTIONS OF THE ROYAL SOCIETY A MATHEMATICAL, PHYSICAL & ENGINEERING SCIENCES